

MPI-H-V 6-1995

Supersymmetry and Neutrinoless Double Beta DecayM. Hirsch¹, H.V. Klapdor-Kleingrothaus²*Max-Planck-Institut für Kernphysik, P.O. 10 39 80, D-69029, Heidelberg,
Germany*S.G. Kovalenko³*Joint Institute for Nuclear Research, Dubna, Russia***Abstract**

Neutrinoless double beta decay ($0\nu\beta\beta$) induced by superparticle exchange is investigated. Such a supersymmetric (SUSY) mechanism of $0\nu\beta\beta$ decay arises within SUSY theories with R-parity non-conservation (\mathcal{R}_p). We consider the minimal supersymmetric standard model (MSSM) with explicit \mathcal{R}_p terms in the superpotential (\mathcal{R}_p MSSM). The decay rate for the SUSY mechanism of $0\nu\beta\beta$ decay is calculated. Numerical values for nuclear matrix elements for the experimentally most interesting isotopes are calculated within pn-QRPA. Constraints on the \mathcal{R}_p MSSM parameter space are extracted from current experimental half-life limits. The most stringent limits are derived from data on ^{76}Ge . It is shown that these constraints are more stringent than those from other low-energy processes and are competitive to or even more stringent than constraints expected from accelerator searches.

1 Introduction

In the standard model (SM), since $B - L$ conservation is exact, neutrinoless double beta decay ($0\nu\beta\beta$), which violates lepton number by two units, is forbidden. On the other hand $B - L$ and L violation is expected in theories

¹MAHIRSCH@ENULL.MPI-HD.MPG.DE

²KLAPDOR@ENULL.MPI-HD.MPG.DE

³KOVALEN@NUSUN.JINR.DUBNA.SU

beyond the SM. That is why $0\nu\beta\beta$ decay has long been recognized as a sensitive tool to put theories beyond the SM to the test (for reviews see [1], [2], [3]). A variety of mechanisms which may cause $0\nu\beta\beta$ have been studied in the past. The simplest and the most well-known possibility is via the exchange of a Majorana neutrino between the decaying neutrons or due to $(B - L)$ -violating right-handed currents. $0\nu\beta\beta$ decay has not yet been seen, but limits on various model parameters can be deduced (see [2], [3] and references therein) from its non-observation.

Recently impressive progress has been achieved in the experimental investigation of double beta decay, both in the $2\nu\beta\beta$ and the $0\nu\beta\beta$ decay mode [4]- [6]. In the near future essential advance in this direction is expected. Experimental lower bounds on $0\nu\beta\beta$ -decay half-lives are often represented in terms of an upper limit on the Majorana neutrino mass $\langle m_\nu \rangle$. At least one experiment currently in operation will reach a final sensitivity of about $\langle m_\nu \rangle = (0.1 - 0.2)$ eV and has already pushed the existing limit below 1 eV [6].

In view of the rising experimental sensitivity it is of great interest to pursue a more comprehensive theoretical study of the possible mechanisms of $0\nu\beta\beta$ decay.

In this work we investigate contributions to $0\nu\beta\beta$ decay within supersymmetric (SUSY) theories with explicit R-parity breaking. R-parity (R_p) is a discrete, multiplicative symmetry defined as $R_p = (-1)^{3B+L+2S}$ [7], where S , B and L are the spin, the baryon and the lepton quantum number. The SM fields, including additional Higgs boson fields appearing in the extended gauge models, have $R_p = +1$ while their superpartners have $R_p = -1$. This symmetry has been imposed on the minimal supersymmetric standard model (MSSM) (for a review see [8]) to ensure baryon number (B) and lepton number (L) conservation. However, neither gauge invariance nor supersymmetry require R_p conservation. The question whether or not R_p is a good symmetry of the supersymmetric theory is a dynamical problem which might be related to more fundamental physics at the Planck scale. In general R_p can be either broken explicitly vacuum expectation value of the scalar superpartner of the R_p -odd isosinglet lepton field [13].

Supersymmetric models with R_p non-conservation (\mathcal{R}_p) have been extensively discussed in the literature not only because of their great theoretical interest, but also because they have interesting phenomenological and cosmological implications.

Existing constraints on \mathcal{R}_p SUSY theories are either direct from collider experiments [14] or indirect from low-energy processes [15], matter stability [16],

[17], [18] and cosmology [19]-[22]. We will discuss the former two constraints later on in more detail in comparison with the bounds from $0\nu\beta\beta$ decay.

Recently \mathcal{R}_p SUSY models have been analysed in connection with current and forthcoming collider experiments. The \mathcal{R}_p SUSY gives rise to spectacular signatures of events in collider detectors which would yield a very clean signal for supersymmetry. Consequently, expected sensitivities of experiments at HERA [25], the TEVATRON [26], LEP 200 [27] and the LHC [28] have been analysed recently. In the present paper we pay special attention to comparing the capability of $0\nu\beta\beta$ decay experiments with the collider experiments in establishing better constraints on \mathcal{R}_p SUSY models.

The rest of the paper is organized as follows. In the next section, we specify the minimal supersymmetric standard model with R_p non-conservation. Section 3 discusses the basic diagrams inducing $0\nu\beta\beta$ decay in the \mathcal{R}_p MSSM. The effective low-energy Lagrangian as well as the different lepton number violating parameters are defined. Section 4 outlines the procedure for obtaining nucleon matrix elements from the quark currents in the non-relativistic impulse approximation. Section 5 then deals with the numerical calculation of the relevant nuclear structure matrix elements. We briefly summarize the main features of the nuclear structure model, before presenting numerical results for those isotopes which are currently the experimentally most promising. Special attention is paid to a discussion of the theoretical uncertainties of the nuclear structure calculation. In section 6, on the basis of the current experimental limit on the half-life of ${}^{76}\text{Ge}$ [6], we analyse constraints on the supersymmetric parameter space imposed by the non-observation of $0\nu\beta\beta$ decay. We have found that these limits are more stringent than those from other low-energy processes and also more stringent than those expected from experiments with the ZEUS detector at HERA [25]. We then close with a short summary and outlook.

2 Minimal Supersymmetric Standard Model with R -parity Non-conservation

In the following we will use the MSSM extended by inclusion of the explicit R -parity non-conserving terms (\mathcal{R}_p) into the superpotential. This model has the MSSM field content and is completely specified by the standard $SU(3) \times SU(2) \times U(1)$ gauge couplings as well as by the low-energy superpotential and "soft" SUSY breaking terms [8]. The most general gauge invariant form of the

superpotential is

$$W = W_{R_p} + W_{\mathcal{R}_p}. \quad (1)$$

The R_p conserving part has the standard MSSM form

$$W_{R_p} = h_L H_1 L \bar{E} + h_D H_1 Q \bar{D} - h_U H_2 Q \bar{U} - \mu H_1 H_2. \quad (2)$$

We use notations L, Q for lepton and quark doublet superfields and $\bar{E}, \bar{U}, \bar{D}$ for lepton and *up*, *down* quark singlet superfields; H_1 and H_2 are the Higgs doublet superfields with a weak hypercharge $Y = -1, +1$, respectively. Summation over generations is implied. For simplicity generation indices of fields and Yukawa coupling constants h_L, h_U, h_D are suppressed. The mass-mixing parameter μ is a free parameter describing mixing between the Higgs bosons H_1 - H_2 as well as between higgsinos \tilde{H}_1 - \tilde{H}_2 .

The R_p violating part of the superpotential (1) can be written as [9], [10],

$$W_{\mathcal{R}_p} = \lambda_{ijk} L_i L_j \bar{E}_k + \lambda'_{ijk} L_i Q_j \bar{D}_k + \lambda''_{ijk} \bar{U}_i \bar{D}_j \bar{D}_k, \quad (3)$$

where indices i, j, k denote generations, and the fields have been defined so that the bilinear lepton number violating operators $L_i H_2$ [10] have been rotated away. The coupling constants λ (λ'') are antisymmetric in the first (last) two indices. The first two terms lead to lepton number violation, while the last one violates baryon number conservation.

Proton stability forbids the simultaneous presence of lepton and baryon number violating terms in the superpotential [16] (unless the couplings are very small). Therefore, only λ, λ' or λ'' type interactions can be present. There may exist an underlying discrete symmetry in the theory which allows either the first or the second set of couplings [17], An example of such a symmetry, which forbids baryon number violating couplings but allows lepton violating ones, is given by the transformation rules [24]

$$(Q, \bar{U}, \bar{D}) \longrightarrow - (Q, \bar{U}, \bar{D}), (L, \bar{E}, H_{1,2}) \longrightarrow + (L, \bar{E}, H_{1,2}). \quad (4)$$

This discrete symmetry can be justified on a more fundamental level of Planck scale physics. It has been shown to be compatible with the ordinary $SU(5)$ [10] and "flipped" $SU(5) \times U(1)$ [31] grand unification (GUT) scenarios as well as with phenomenologically viable superstring theories [32].

Neutrinoless double beta decay, which is the main subject of the present paper, requires lepton number violating interactions. Therefore we bind ourselves to the \mathcal{R}_p MSSM with lepton number violation ($\lambda \neq 0, \lambda' \neq 0$) and

baryon number conservation ($\lambda'' = 0$). The Lagrangian of this model possesses the discrete symmetry eq. (4). Apparently, $0\nu\beta\beta$ can probe only the first generation lepton number violating coupling λ'_{111} because only the first generation fermions u, d, e are involved in this process.

In addition to proton decay constraints on \mathbb{R}_p couplings there are also constraints which follow from cosmological arguments, requiring that the baryon asymmetry generated at the GUT scale is not washed out by $B - L$ violating interactions present in eq. (3). These cosmological constraints have been thought to affect all \mathbb{R}_p couplings $\lambda, \lambda', \lambda'' \ll 10^{-7}$, making these models phenomenologically not interesting. These arguments, however, were proved to be strongly model dependent [21], bounds can be evaded in perfectly reasonable scenarios of matter genesis [22].

The effect of "soft" supersymmetry breaking can be parametrized at the Fermi scale as a part of the scalar potential:

$$V_{soft} = \sum_{i=scalar} m_i^2 |\phi_i|^2 + h_L A_L H_1 \tilde{L} \tilde{E} + h_D A_D H_1 \tilde{Q} \tilde{D} - h_U A_U H_2 \tilde{Q} \tilde{U} - \mu B H_1 H_2 + \text{h.c.} \quad (5)$$

and a "soft" gaugino mass term

$$\mathcal{L}_{GM} = -\frac{1}{2} [M_1 \tilde{B} \tilde{B} + M_2 \tilde{W}^k \tilde{W}^k + M_3 \tilde{g}^a \tilde{g}^a] - \text{h.c.} \quad (6)$$

As usual, $M_{3,2,1}$ are the masses of the $SU(3) \times SU(2) \times U(1)$ gauginos $\tilde{g}, \tilde{W}, \tilde{B}$ and m_i are the masses of scalar fields. A_L, A_D, A_U and B are trilinear and bilinear "soft" supersymmetry breaking parameters. All these quantities are free SUSY model parameters which due to the renormalization effect depend on the energy scale Λ .

Considering a GUT scenario within the MSSM one can claim the following unification conditions at the GUT scale $\Lambda \sim M_X$:

$$A_U(M_X) = A_D(M_X) = A_L(M_X) = A_0, \quad (7)$$

$$m_L(M_X) = m_E(M_X) = m_Q(M_X) = m_U(M_X) = m_D(M_X) = m_0, \quad (8)$$

$$M_1(M_X) = M_2(M_X) = M_3(M_X) = m_{1/2}, \quad (9)$$

$$g_1(M_X) = g_2(M_X) = g_3(M_X) = g_{GUT}, \quad (10)$$

where g_3, g_2, g_1 are the $SU(3) \times SU(2) \times U(1)$ gauge coupling constants equal to g_{GUT} at the unification scale M_X .

At the Fermi scale $\Lambda \sim M_W$ these parameters can be evaluated on the basis of the MSSM renormalization group equations (RGE) [33],[34]. We assume that the \mathcal{R}_p Yukawa coupling constants $\lambda, \lambda', \lambda''$ are small enough to be neglected in these equations. Equation (9) implies at $\Lambda \sim M_W$

$$M_1 = \frac{5}{3} \tan^2 \theta_W \cdot M_2, \quad M_2 \simeq 0.3 m_{\tilde{g}}. \quad (11)$$

Here $m_{\tilde{g}} = M_3$ is the gluino mass.

Now the model is completely specified and we can deduce the interaction terms of the \mathcal{R}_p MSSM - Lagrangian relevant for neutrinoless double beta decay.

Write down these interaction terms explicitly. Note that in the following we use for fermion fields the 4-component Dirac bispinor notation.

The lepton number violating part of the Lagrangian can be obtained directly from the superpotential (3). It has the form

$$\begin{aligned} \mathcal{L}_{\mathcal{R}_p} = & - \lambda'_{111} \left[(\bar{u}_L \bar{d}_R) \cdot \begin{pmatrix} e_R^c \\ -\nu_R^c \end{pmatrix} \tilde{d}_R + (\bar{e}_L \bar{\nu}_L) d_R \cdot \begin{pmatrix} \tilde{u}_L^* \\ -\tilde{d}_L^* \end{pmatrix} + \right. \\ & \left. + (\bar{u}_L \bar{d}_L) d_R \cdot \begin{pmatrix} \tilde{e}_L^* \\ -\tilde{\nu}_L^* \end{pmatrix} + h.c. \right] \end{aligned} \quad (12)$$

The Lagrangian terms corresponding to gluino $\mathcal{L}_{\tilde{g}}$ and neutralino \mathcal{L}_χ interactions with fermions $\psi = \{u, d, e\}$, $q = \{u, d\}$ and their superpartners $\tilde{\psi} = \{\tilde{u}, \tilde{d}, \tilde{e}\}$, $\tilde{q} = \{\tilde{u}, \tilde{d}\}$ are [8]

$$\mathcal{L}_{\tilde{g}} = -\sqrt{2} g_3 \frac{\lambda_{\alpha\beta}^{(a)}}{2} \left(\bar{q}_L^\alpha \tilde{g} \tilde{q}_L^\beta - \bar{q}_R^\alpha \tilde{g} \tilde{q}_R^\beta \right) + h.c., \quad (13)$$

$$\mathcal{L}_\chi = \sqrt{2} g_2 \sum_{i=1}^4 \left(\epsilon_{Li}(\psi) \bar{\psi}_L \chi_i \tilde{\psi}_L + \epsilon_{Ri}(\psi) \bar{\psi}_R \chi_i \tilde{\psi}_R \right) + h.c. \quad (14)$$

Here $\lambda^{(a)}$ are 3×3 Gell-Mann matrices ($a = 1, \dots, 8$). Neutralino coupling constants are defined as [8]

$$\epsilon_{Li}(\psi) = -T_3(\psi) \mathcal{N}_{i2} + \tan \theta_W (T_3(\psi) - Q(\psi)) \mathcal{N}_{i1}, \quad (15)$$

$$\epsilon_{Ri}(\psi) = Q(\psi) \tan \theta_W \mathcal{N}_{i1}. \quad (16)$$

Here $Q(\psi)$ and $T_3(\psi)$ are the electric charge and weak isospin of the field ψ .

Coefficients N_{ij} are elements of the orthogonal neutralino mixing matrix which diagonalizes the neutralino mass matrix. In the \mathbb{R}_p MSSM the neutralino mass matrix is identical to the MSSM one [8] and in the basis of fields $(\tilde{B}, \tilde{W}^3, \tilde{H}_1^0, \tilde{H}_2^0)$ has the form:

$$M_\chi = \begin{pmatrix} M_1 & 0 & -M_Z s_W c_\beta & M_Z s_W s_\beta \\ 0 & M_2 & M_Z c_W c_\beta & -M_Z c_W s_\beta \\ -M_Z s_W c_\beta & M_Z c_W c_\beta & 0 & -\mu \\ M_Z s_W s_\beta & -M_Z c_W s_\beta & -\mu & 0 \end{pmatrix}, \quad (17)$$

where $c_W = \cos \theta_W$, $s_W = \sin \theta_W$, $t_W = \tan \theta_W$, $s_\beta = \sin \beta$, $c_\beta = \cos \beta$. The angle β is defined as $\tan \beta = \langle H_2^0 \rangle / \langle H_1^0 \rangle$. Here $\langle H_2^0 \rangle$ and $\langle H_1^0 \rangle$ are vacuum expectation values of the neutral components H_2^0 and H_1^0 of the Higgs doublet fields with weak hypercharges $Y(H_2^0) = +1$ and $Y(H_1^0) = -1$, respectively. The mass parameters M_1, M_2 are related to the gluino mass $m_{\tilde{g}}$ according to eq. (11).

By diagonalizing the mass matrix (17) one can obtain four neutralinos χ_i with masses m_{χ_i} and the field content

$$\chi_i = \mathcal{N}_{i1} \tilde{B} + \mathcal{N}_{i2} \tilde{W}^3 + \mathcal{N}_{i3} \tilde{H}_1^0 + \mathcal{N}_{i4} \tilde{H}_2^0. \quad (18)$$

Recall again that we use notations \tilde{W}^3, \tilde{B} for neutral $SU(2)_L \times U(1)$ gauginos and $\tilde{H}_2^0, \tilde{H}_1^0$ for higgsinos which are the superpartners of the two neutral Higgs boson fields H_1^0 and H_2^0 .

We apply a diagonalization by means of a real orthogonal matrix \mathcal{N} . Therefore the coefficients \mathcal{N}_{ij} are real and masses m_{χ_i} are either positive or negative. The sign of the mass coincides with the CP-parity of the corresponding neutralino mass eigenstate χ_i . If necessary, a negative mass can be always made positive by a redefinition [35] of the neutralino field χ_i . It leads to a redefinition of the relevant mixing coefficients $\mathcal{N}_{ij} \rightarrow i \cdot \mathcal{N}_{ij}$.

The lightest neutralino is commonly assumed to be the lightest supersymmetric particle (LSP). That is true in almost all phenomenologically viable SUSY models with R_p conservation. For \mathbb{R}_p SUSY models this is a very non-trivial assumption, since the cosmological constraints [36] requiring the LSP to be colour and electrically neutral, no longer apply [20]. A priori, the LSP could be any superparticle in \mathbb{R}_p SUSY models. However, the RGE analysis in minimal supergravity models suggests that the LSP is a neutralino if \mathbb{R}_p couplings are reasonably small the lightest neutralino. If R_p is conserved the LSP is a stable particle. Otherwise it decays into ordinary matter.

Squarks $\tilde{u}_{L,R}$, $\tilde{d}_{L,R}$ and selectron $\tilde{e}_{L,R}$ in eqs. (13), (14) are with a good precision mass eigenstates. Possible $\tilde{f}_L - \tilde{f}_R$ -mixing for the first generation of squarks and sleptons are negligible due to the smallness of the relevant Yukawa couplings. In this case the MSSM mass formulas can be written as [8], [33] [34]

$$m_{\tilde{e}_L}^2 = m_0^2 + 0.07m_{\tilde{g}}^2 + \frac{1}{2} \cos 2\beta M_Z^2 (2 \sin^2 \theta_W - 1), \quad (19)$$

$$m_{\tilde{e}_R}^2 = m_0^2 + 0.02m_{\tilde{g}}^2 - \cos 2\beta M_Z^2 \sin^2 \theta_W, \quad (20)$$

$$m_{\tilde{u}_L}^2 = m_0^2 + 0.83m_{\tilde{g}}^2 + \frac{1}{2} \cos 2\beta M_Z^2 (1 - \frac{4}{3} \sin^2 \theta_W), \quad (21)$$

$$m_{\tilde{d}_L}^2 = m_0^2 + 0.83m_{\tilde{g}}^2 - \frac{1}{2} \cos 2\beta M_Z^2 (1 - \frac{2}{3} \sin^2 \theta_W), \quad (22)$$

$$m_{\tilde{u}_R}^2 = m_0^2 + 0.77m_{\tilde{g}}^2 + \cos 2\beta M_Z^2 \frac{2}{3} \sin^2 \theta_W, \quad (23)$$

$$m_{\tilde{d}_R}^2 = m_0^2 + 0.76m_{\tilde{g}}^2 - \cos 2\beta M_Z^2 \frac{1}{3} \sin^2 \theta_W. \quad (24)$$

Here, $m_{\tilde{g}}$ is the gluino mass and m_0 is the common sfermion mass at the unification scale (see (8)). From the eqs. (19)-(24) one can estimate in the region $m_{\tilde{u}_L}^2, m_{\tilde{d}_R}^2 \lesssim 300 \text{ GeV}$ that $m_{\tilde{u}_L}^2 \approx m_{\tilde{d}_R}^2$. This approximate relation will be helpful for understanding the results of our numerical analysis in Sect. 6.

Having specified the Lagrangian interaction terms (12) - (14) and the mass eigenstates $\tilde{g}, \chi_i, \tilde{q}, \tilde{e}$ involved in the interactions we can construct diagrams describing the \mathcal{R}_p MSSM contribution to the neutrinoless double beta decay.

In principle, in the \mathcal{R}_p MSSM a small neutrino mass of Majorana type may arise radiatively [10], [37]. On the other hand in some GUT scenarios based on large gauge groups like $SO(10)$ there might be also heavy Majorana fermions having non-negligible $SU(2)_L$ components. It is often identified with the heavy Majorana neutrino N . In the presence of either the light Majorana neutrinos or the heavy ones (or both) $0\nu\beta\beta$ decay can be induced by the conventional neutrino mass mechanism. In the present paper we concentrate on the \mathcal{R}_p SUSY mechanism of $0\nu\beta\beta$ decay. The effect of additional contributions from the neutrino mass mechanism is investigated in the case of heavy Majorana neutrino exchange. (Inclusion of the light Majorana neutrino contribution will not change the results of our analysis.)

3 Low-energy $\Delta L_e = 2$ - Effective Lagrangian

The basic diagram corresponding to the neutrinoless double beta decay at the nucleon level is presented in fig.1(a). Two neutrons from the initial nucleus A_i after interaction transform into two protons of the final nucleus A_f emitting two electrons. Apparently this process breaks the electron lepton number by two units, $\Delta L_e = 2$. At the quark level it can be induced by the subprocess with two initial d-quarks and two final u-quarks accompanied by two electrons as shown in Fig 1(b).

The conventional mass mechanism with Majorana neutrino exchange is presented in fig. 2(a). In the following we consider the \mathcal{R}_p MSSM contribution to $0\nu\beta\beta$ decay. Starting from the fundamental interactions (12)-(14) we have found [38] the complete set of diagrams presented in fig. 2(b, c) which contribute to this subprocess.

The supersymmetric mechanism of $0\nu\beta\beta$ decay was first proposed by Mohapatra [39] and later studied in more details by Vergados [40]. In these papers [39], [40] only three diagrams similar to those in fig.2(b) were considered. Instead of neutralinos χ_i , which are actual mass eigenstates in the MSSM, the consideration of refs. [39], [40] used Z-ino (\tilde{Z}) and photino ($\tilde{\gamma}$) fields in intermediate states. \tilde{Z} and $\tilde{\gamma}$ can be mass eigenstates only at special values of parameters of the neutralino mass matrix. In general, these fields are not mass eigenstates. Furthermore, it was recently realized that a cosmologically viable lightest neutralino is very likely B-ino dominant [41]. Using in the intermediate states such fields which are not mass eigenstates leads to neglecting diagrams with mixed intermediate states when, for instance, \tilde{Z} turns to $\tilde{\gamma}$ due to the mixing proportional to the relevant entry of the neutralino mass matrix. The effect of mixing is taken into account completely in the set of diagrams displayed in fig.2(b,c) with all neutralino mass eigenstates χ_i involved.

In the case of $0\nu\beta\beta$ decay when momenta of external particles are much smaller than intermediate particle masses one can treat interactions in fig. 1(b) and fig. 2 as point-like. A suitable formalism in this case is the effective Lagrangian approach.

Define the effective Lagrangian $\mathcal{L}_{eff}^{\Delta L_e=2}(x)$ as

$$\begin{aligned} \langle f|S - 1|i \rangle &= i \int d^4x \langle f|\mathcal{L}_{eff}^{\Delta L_e=2}(x)|i \rangle + \\ &+ \text{high orders of perturbation theory.} \end{aligned} \quad (25)$$

Thus, $\mathcal{L}_{eff}^{\Delta L_e=2}(x)$ corresponds to the lowest order operator structure having

non-vanishing matrix elements of the form

$$\langle uuee | \mathcal{L}_{eff}^{\Delta L_e=2}(x) | dd \rangle \neq 0. \quad (26)$$

It is now straightforward to find the operators in the effective Lagrangian which correspond to the diagrams in fig. 2(b,c). The result is [38]

$$\begin{aligned} \mathcal{L}_{eff}^{\Delta L_e=2}(x) = & 8\pi\alpha_2\lambda'_{111} \sum_{i=1}^4 \frac{1}{m_{\chi_i}} \left[\frac{\epsilon_{Li}^2(e)}{m_{\tilde{e}_L}^4} (\bar{u}_L^\alpha d_{R\alpha}) (\bar{u}_L^\beta d_{R\beta}) (\bar{e}_L e_R^c) + \right. & (27) \\ & + \frac{\epsilon_{Li}^2(u)}{m_{\tilde{u}_L}^4} (\bar{u}_L^\alpha u_{R\beta}^c) (\bar{e}_L d_{R\alpha}) (\bar{e}_L d_R^\beta) + \frac{\epsilon_{Ri}^2(d)}{m_{\tilde{d}_R}^4} (\bar{u}_L^\alpha e_R^c) (\bar{u}_L^\beta e_R^c) (\bar{d}^c_{L\alpha} d_{R\beta}) + \\ & + \left. \left(\frac{\epsilon_{Li}(u)\epsilon_{Ri}(d)}{m_{\tilde{u}_L}^2 m_{\tilde{d}_R}^2} + \frac{\epsilon_{Li}(u)\epsilon_{Li}(e)}{m_{\tilde{u}_L}^2 m_{\tilde{e}_L}^2} + \frac{\epsilon_{Li}(e)\epsilon_{Ri}(d)}{m_{\tilde{e}_L}^2 m_{\tilde{d}_R}^2} \right) (\bar{u}_L^\alpha d_R^\beta) (\bar{u}_{L\beta} e_R^c) (\bar{e}_L d_{R\alpha}) \right] + \\ & + \lambda'_{111} \frac{8\pi\alpha_s}{m_{\tilde{g}}} \frac{\lambda_{\alpha\beta}^{(a)}}{2} \frac{\lambda_{\gamma\delta}^{(a)}}{2} \left[\frac{1}{m_{\tilde{u}_L}^4} (\bar{u}_L^\alpha u_R^c) (\bar{e}_L d_R^\beta) (\bar{e}_L d_R^\delta) + \right. \\ & + \left. \frac{1}{m_{\tilde{d}_R}^4} (\bar{u}_L^\alpha e_R^c) (\bar{u}_L^\gamma e_R^c) (\bar{d}^c_{L\beta} d_R^c{}^\delta) - \frac{1}{m_{\tilde{d}_R}^2 m_{\tilde{u}_L}^2} (\bar{u}_L^\alpha d_R^\delta) (\bar{u}_L^\gamma e_R^c) (\bar{e}_L d_R^\beta) \right] \end{aligned}$$

Gauge coupling constants $\alpha_2 = g_2^2/(4\pi)$ and $\alpha_s = g_3^2/(4\pi)$ are running coupling constants which should be estimated at the proper energy scale Λ . One can see from the diagrams in fig.2 that the typical scale at which the $\tilde{g} - \tilde{q} - q$ and $\chi - \tilde{q} - q$ interactions occur is of the order of the gluino or neutralino mass. In the mass region which will be analysed numerically in the subsequent sections we may take approximately these couplings at the Z-boson pole and use their values from ref. [42]:

$$\alpha_s(M_Z) = 0.127, \quad \alpha_2(M_Z) = 0.0337. \quad (28)$$

The Lagrangian (27) has terms in a form which do not allow a direct application of the non-relativistic impulse approximation for further calculation of the $0\nu\beta\beta$ reaction matrix element. One should rearrange the right hand side of eq. (27) in the form of a product of two colour-singlet quark currents and the leptonic current. It can be accomplished by a Fierz rearrangement procedure and subsequent extraction of color-singlets from the product of two colour-triplet and colour-antitriplet quark fields. The final result is

$$\mathcal{L}_{eff}^{\Delta L_e=2}(x) = \frac{G_F^2}{2} \cdot m_P^{-1} \left[(\eta_{\tilde{g}} + \eta_\chi) (J_{PS} J_{PS} - \frac{1}{4} J_T^{\mu\nu} J_{T\mu\nu}) + \right. \quad (29)$$

$$+ (\eta_{\chi\bar{e}} + \eta'_{\bar{g}} - \eta_{\chi\bar{f}})J_{PS}J_{PS} + \eta_N J_{VA}^\mu J_{VA\mu}] (\bar{e}(1 + \gamma_5)e^c),$$

The last term corresponds to the heavy Majorana neutrino contribution described by the diagram in fig. 2(a) which we also consider in the present paper as discussed at the end of section 2.

The lepton number violating parameters are defined as follows

$$\eta_{\bar{g}} = \frac{2\pi\alpha_s}{9} \frac{\lambda'_{111}{}^2}{G_F^2 m_{\bar{d}_R}^4} \frac{m_P}{m_{\bar{g}}} \left[1 + \left(\frac{m_{\bar{d}_R}}{m_{\bar{u}_L}} \right)^4 \right] \quad (30)$$

$$\eta_{\chi} = \frac{\pi\alpha_2}{6} \frac{\lambda'_{111}{}^2}{G_F^2 m_{\bar{d}_R}^4} \sum_{i=1}^4 \frac{m_P}{m_{\chi_i}} \left[\epsilon_{Ri}^2(d) + \epsilon_{Li}^2(u) \left(\frac{m_{\bar{d}_R}}{m_{\bar{u}_L}} \right)^4 \right] \quad (31)$$

$$\eta_{\chi\bar{e}} = 2\pi\alpha_2 \frac{\lambda'_{111}{}^2}{G_F^2 m_{\bar{d}_R}^4} \left(\frac{m_{\bar{d}_R}}{m_{\bar{e}_L}} \right)^4 \sum_{i=1}^4 \epsilon_{Li}^2(e) \frac{m_P}{m_{\chi_i}}, \quad (32)$$

$$\eta'_{\bar{g}} = \frac{4\pi\alpha_s}{9} \frac{\lambda'_{111}{}^2}{G_F^2 m_{\bar{d}_R}^4} \frac{m_P}{m_{\bar{g}}} \left(\frac{m_{\bar{d}_R}}{m_{\bar{u}_L}} \right)^2, \quad (33)$$

$$\eta_{\chi\bar{f}} = \frac{\pi\alpha_2}{3} \frac{\lambda'_{111}{}^2}{G_F^2 m_{\bar{d}_R}^4} \left(\frac{m_{\bar{d}_R}}{m_{\bar{e}_L}} \right)^2 \sum_{i=1}^4 \frac{m_P}{m_{\chi_i}} [\epsilon_{Ri}(d)\epsilon_{Li}(e) + \epsilon_{Li}(u)\epsilon_{Ri}(d) \left(\frac{m_{\bar{e}_L}}{m_{\bar{u}_L}} \right)^2 + \epsilon_{Li}(u)\epsilon_{Li}(e) \left(\frac{m_{\bar{d}_R}}{m_{\bar{u}_L}} \right)^2], \quad (34)$$

$$\eta_N = \frac{m_P}{\langle m_N \rangle}, \quad (35)$$

where $\langle m_N \rangle$ is the *effective* heavy Majorana neutrino mass (for definition see [3]).

Colour-singlet hadronic currents have the form

$$J_{PS} = \bar{u}^\alpha(1 + \gamma_5)d_\alpha, \quad (36)$$

$$J_T^{\mu\nu} = \bar{u}^\alpha\sigma^{\mu\nu}(1 + \gamma_5)d_\alpha, \quad (37)$$

$$J_{AV}^\mu = \bar{u}^\alpha\gamma^\mu(1 - \gamma_5)d_\alpha, \quad (38)$$

where $\sigma^{\mu\nu} = \frac{i}{2}[\gamma^\mu, \gamma^\nu]$.

Now we can consider nucleon matrix elements of these quark currents which provide us with certain information about quark states in the nucleon. Further we will use in Sect. 5 the proper nuclear wave functions to describe nucleon states in the nucleus. Applying this standard two-step-procedure we will obtain the reaction matrix element for the $0\nu\beta\beta$ decay.

4 From quark to nuclear level

Adopting the above mentioned two-step-procedure let us write down the $0\nu\beta\beta$ decay matrix element $\mathcal{R}_{0\nu\beta\beta}$ corresponding to the effective Lagrangian eq. (29). Using the general formula eq. (86) one can write

$$\mathcal{R}_{0\nu\beta\beta} = \frac{G_F^2}{\sqrt{2}} m_P^{-1} C_{0\nu}^{-1} \{ \bar{e}(1 + \gamma_5)e^c \} \times \quad (39)$$

$$\left[(\eta_{\tilde{g}} + \eta_\chi) \langle F | \Omega_{\tilde{q}} | I \rangle + (\eta_{\chi\tilde{e}} + \eta'_{\tilde{g}} - \eta_{\chi\tilde{f}}) \langle F | \Omega_{\tilde{f}} | I \rangle + \eta_N \langle F | \Omega_N | I \rangle \right].$$

The heavy Majorana neutrino exchange contribution has been included in the last term of this equation. It corresponds to the last term of eq. (29).

We have introduced transition operators Ω_i (see eq. (87) in Appendix) which are useful for separating the particle physics part of the calculation from the nuclear physics one. The transition operators contain information about the underlying interactions at the quark level (29) and quark states inside the nucleon. They are independent of the initial $|I\rangle$ and the final $\langle F|$ nuclear states. To calculate the nuclear matrix elements in eq. (39) one should use nuclear model wave functions.

Nuclear matrix elements of the transition operators $\Omega_{\tilde{q}}, \Omega_{\tilde{f}}$ and Ω_N describe transitions induced by quark colour singlet currents (36)-(38) in the first, second and third terms of eq. (29). Diagrams in fig. 2 with the intermediate states $\{W - N - W\}$, $\{\tilde{u}(\tilde{d}) - \chi, \tilde{g} - \tilde{u}(\tilde{d})\}$ and $\{\tilde{u}(\tilde{d}) - \chi, \tilde{g} - \tilde{d}(\tilde{u}); \tilde{e} - \chi - \tilde{e}, \tilde{q}\}$ contribute to operators $\Omega_N, \Omega_{\tilde{q}}$ and $\Omega_{\tilde{f}}$, respectively.

The relevant formula for calculating the transition operators in the non-relativistic impulse approximation (NRIA) (89) require the nucleon matrix elements of these currents.

Now we turn to the derivation of nucleon matrix elements of the colour singlet quark currents (36)-(38) using results of ref. [43]. The relevant matrix elements are,

$$\langle P(p) | \bar{u}d | N(p') \rangle = F_S^{(3)}(q^2) \cdot \bar{N}(p) \tau_+ N(p'), \quad (40)$$

$$\langle P(p) | \bar{u}\gamma_5 d | N(p') \rangle = F_P^{(3)}(q^2) \cdot \bar{N}(p) \gamma_5 \tau_+ N(p'), \quad (41)$$

$$\langle P(p) | \bar{u}\sigma^{\mu\nu}(1 + \gamma_5)d | N(p') \rangle = \bar{N}(p) \left(J^{\mu\nu} + \frac{i}{2} \epsilon^{\mu\nu\rho\sigma} J_{\rho\sigma} \right) \tau_+ N(p'), \quad (42)$$

$$\langle P(p) | \bar{u}\gamma^\mu(1 - \gamma_5)d | N(p') \rangle = \bar{N}(p) \gamma^\mu \left(F_V(q^2) - F_A(q^2) \gamma_5 \right) \tau_+ N(p') \quad (43)$$

where $q = p - p'$ and the tensor structure is defined as

Table 1: Nucleon form factor normalizations (at $q^2 = 0$) as calculated in [43].

Set	$F_S^{(3)}$	$F_P^{(3)}$	$T_1^{(3)}$	$T_2^{(3)}$	$T_3^{(3)}$
A) Bag Model	0.48	4.41	1.38	-3.30	-0.62
B) Non-relativistic quark model	0.62	4.65	1.45	-1.48	-0.66

$$J^{\mu\nu} = T_1^{(3)}(q^2)\sigma^{\mu\nu} + \frac{iT_2^{(3)}}{m_P}(\gamma^\mu q^\nu - \gamma^\nu q^\mu) + \frac{T_3^{(3)}}{m_P^2}(\sigma^{\mu\rho}q_\rho q^\nu - \sigma^{\nu\rho}q_\rho q^\mu). \quad (44)$$

For all form factors $F_{V,A}(q^2)$, $F_{S,P}^{(3)}(q^2)$, $T_i^{(3)}(q^2)$ we take following ref. [44] a dipole form

$$\frac{F_{V,A}(q^2)}{f_{V,A}} = \frac{F_{S,P}^{(3)}(q^2)}{F_{S,P}^{(3)}(0)} = \frac{T_i^{(3)}(q^2)}{T_i^{(3)}(0)} = \left(1 - \frac{q^2}{m_A^2}\right)^{-2} \quad (45)$$

with $m_A = 0.85\text{GeV}$ and $f_V \approx 1$, $f_A \approx 1.261$. Form factor normalization values $F_{S,P}^{(3)}(0)$, $T_i^{(3)}(0)$ were calculated in ref. [43] and are given in Table 1.

Using formulas (40)-(44) we may derive the non-relativistic limit $m_P \gg |\vec{p}|$ for nucleon matrix elements of the three combinations of the quark currents in (29). Keeping all terms up to order q^2 in the non-relativistic expansion we find from eq. (89) the relevant transition operators $\Omega_{\bar{q}}$, $\Omega_{\bar{f}}$, Ω_N for two outgoing electrons in the S-wave state,

$$\Omega_{\bar{q}} = \frac{m_P}{m_e} \left\{ \alpha_V^{(0)} \Omega_{F,N} + \alpha_A^{(0)} \Omega_{GT,N} + \alpha_V^{(1)} \Omega_{F'} + \alpha_A^{(1)} \Omega_{GT'} + \alpha_T \Omega_{T'} \right\}, \quad (46)$$

$$\Omega_{\bar{f}} = \Omega_{\bar{q}}(T_i = 0), \quad (47)$$

$$\Omega_N = \frac{m_P}{m_e} \left\{ \left(\frac{f_V}{f_A}\right)^2 \Omega_{F,N} - \Omega_{GT,N} \right\}, \quad (48)$$

where partial transition operators are

$$\Omega_{GT,N} = \sum_{i \neq j} \tau_+^{(i)} \tau_+^{(j)} \boldsymbol{\sigma}_i \cdot \boldsymbol{\sigma}_j \left(\frac{R_0}{r_{ij}}\right) F_N(x_A), \quad (49)$$

$$\Omega_{F,N} = \sum_{i \neq j} \tau_+^{(i)} \tau_+^{(j)} \left(\frac{R_0}{r_{ij}}\right) F_N(x_A), \quad (50)$$

$$\Omega_{GT'} = \sum_{i \neq j} \tau_+^{(i)} \tau_+^{(j)} \boldsymbol{\sigma}_i \cdot \boldsymbol{\sigma}_j \left(\frac{R_0}{r_{ij}} \right) F_4(x_A), \quad (51)$$

$$\Omega_{F'} = \sum_{i \neq j} \tau_+^{(i)} \tau_+^{(j)} \left(\frac{R_0}{r_{ij}} \right) F_4(x_A), \quad (52)$$

$$\Omega_{T'} = \sum_{i \neq j} \tau_+^{(i)} \tau_+^{(j)} \{3(\boldsymbol{\sigma}_i \cdot \hat{\mathbf{r}}_{ij})(\boldsymbol{\sigma}_j \cdot \hat{\mathbf{r}}_{ij}) - \boldsymbol{\sigma}_i \cdot \boldsymbol{\sigma}_j\} \left(\frac{R_0}{r_{ij}} \right) F_5(x_A). \quad (53)$$

Here, R_0 is the nuclear radius, introduced to make the matrix elements dimensionless (compensating factors have been absorbed into the phase space integrals [3]). The following notations are used

$$\mathbf{r}_{ij} = (\vec{r}_i - \vec{r}_j), \quad r_{ij} = |\mathbf{r}_{ij}|, \quad \hat{\mathbf{r}}_{ij} = \mathbf{r}_{ij}/r_{ij}, \quad x_A = m_A r_{ij}.$$

Here \vec{r}_i is the coordinate of the "ith" nucleon. The above matrix elements have been written in the closure approximation, which is well satisfied due to the large masses of the intermediate particles.

The nucleon structure coefficients in (46) are given by

$$\alpha_V^{(0)} = \left(\frac{F_S^{(3)}}{f_A} \right)^2, \quad \alpha_A^{(0)} = - \left(\frac{T_1^{(3)}}{f_A} \right)^2, \quad (54)$$

$$\alpha_V^{(1)} = - \left(\frac{m_A}{m_P} \right)^2 \alpha_A^{(0)} \left[\frac{1}{4} + \left(\frac{T_2^{(3)}}{T_1^{(3)}} \right)^2 - \frac{T_2^{(3)}}{T_1^{(3)}} \right], \quad (55)$$

$$\alpha_A^{(1)} = - \left(\frac{m_A}{m_P} \right)^2 \left[\alpha_A^{(0)} \left(\frac{1}{6} - \frac{2T_2^{(3)}}{3T_1^{(3)}} + \frac{4T_3^{(3)}}{3T_1^{(3)}} \right) + \frac{1}{12} \left(\frac{F_P^{(3)}}{f_A} \right)^2 \right], \quad (56)$$

$$\alpha_T = - \left(\frac{m_A}{m_P} \right)^2 \left[\alpha_A^{(0)} \left(\frac{1}{12} - \frac{1T_2^{(3)}}{3T_1^{(3)}} + \frac{2T_3^{(3)}}{3T_1^{(3)}} \right) - \frac{1}{12} \left(\frac{F_P^{(3)}}{f_A} \right)^2 \right]. \quad (57)$$

Here $F_{S,P}^{(3)} \equiv F_{S,P}^{(3)}(0)$, $T_i^{(3)} \equiv T_i^{(3)}(0)$.

Three different structure functions F_i appear in eqs. (49)-(53) (we use notations of ref. [40]). They are given by the integrals over the momentum \mathbf{q} transferred between two nucleons (see eq. (89))

$$F_N(x_A) = 4\pi m_A^6 r_{ij} \int \frac{d^3 \mathbf{q}}{(2\pi)^3} \frac{1}{(m_A^2 + \mathbf{q}^2)^4} e^{i\mathbf{q}\mathbf{r}_{ij}} \quad (58)$$

$$F_4(x_A) = 4\pi m_A^4 r_{ij} \int \frac{d^3 \mathbf{q}}{(2\pi)^3} \frac{\mathbf{q}^2}{(m_A^2 + \mathbf{q}^2)^4} e^{i\mathbf{q}\mathbf{r}_{ij}} \quad (59)$$

$$F_5(x_A) = 2\pi m_A^4 r_{ij} \int \frac{d^3 \mathbf{q}}{(2\pi)^3} \frac{\mathbf{q}^2 - \frac{1}{3}(\mathbf{q} \cdot \hat{\mathbf{r}}_{ij})^2}{(m_A^2 + \mathbf{q}^2)^4} e^{i\mathbf{q}\mathbf{r}_{ij}}. \quad (60)$$

These functions are analogous to the "neutrino potentials" for the case of the light Majorana neutrino exchange. Nuclear energy denominators typical for such momentum integrals can be neglected safely from eqs. (58)-(60) in the case of heavy intermediate particles, such as SUSY particles and the heavy Majorana neutrino N , with masses much larger than the characteristic nuclear energy and are therefore suppressed in (58)-(60). The analytic solutions of the integrals in eqs. (58)-(60) are

$$F_N(x) = \frac{x}{48}(3 + 3x + x^2)e^{-x}, \quad F_4(x) = \frac{x}{48}(3 + 3x - x^2)e^{-x}, \quad (61)$$

$$F_5(x) = \frac{x^3}{48}e^{-x}.$$

At this stage we point out that our formulas for the coefficients (54)-(57) of the transition operators (46)-(47) disagree with the corresponding formulas derived in ref. [40]. Particularly, in our case $\alpha_A^{(0)} \leq 0$ while in ref. [40] this coefficient is positive. This sign difference has an important consequence if one considers simultaneously the supersymmetric and the heavy Majorana neutrino contributions. It will be seen in the next section that in both the neutrino exchange and in the \mathcal{R}_p SUSY mechanisms the dominant contributions correspond to the $\Omega_{GT,N}$ transition operator, initiating Gamow-Teller $0^+ \rightarrow 0^+$ nuclear transitions. Comparing eq. (46) with eq. (48) one can see that our formulas correspond to a constructive interference between the dominant $\Omega_{GT,N}$ terms of these two mechanisms while formulas from ref. [40] correspond to a destructive one. In the latter case both contributions can cancel each other and by a proper choice of λ'_{111} in (30)-(34) the matrix element of $0\nu\beta\beta$ -decay can be set to zero at any values of particle masses involved in the formulas. As a result the $0\nu\beta\beta$ -decay half-life limit would neither constrain supersymmetric particle masses nor that for Majorana neutrinos. Our formulas (46), (47) and (54)-(57) always lead to certain constraints on these masses. We return to a detailed discussion of this point in section 6.

5 Nuclear matrix elements in the pn-QRPA approach

While the formalism of the SUSY $0\nu\beta\beta$ decay outlined in the previous sections is independent of the nuclear structure model used to generate the wave functions, numerical values of matrix elements are model dependent. We therefore separate this part of our work from the rest of the formalism in order to split up nuclear and particle physics uncertainties in a most distinctive way.

5.1 Basic summary of the nuclear model and its parameters

Nuclear matrix elements have been calculated within pn-QRPA (proton - neutron Quasiparticle Random Phase Approximation). pn-QRPA, the RPA for charge-changing transitions has been developed by Halbleib and Sorenson [45] and during recent years widely been applied to double beta decay calculations [46]- [52]. In the present work we follow essentially the description of [49], [50], [52].

Further we just briefly summarize the numerically most important features.

We account for typically two major oscillator shells, for example $3\hbar\omega$ and $4\hbar\omega$ in case of ^{76}Ge . Single particle energies are calculated from a Coulomb-corrected Woods-Saxon potential with Bohr-Mottelson parameters [53], except that the strength of the spin-orbit force has been reduced according to [52] by $\sim 9\%$ for a better agreement with experimental data. For the pairing (in Bardeen-Cooper-Schrieffer (BCS) approximation) and RPA calculation we used consistently the Paris nucleon-nucleon potential [54]. The strengths of the pairing interactions in the BCS calculation have been adjusted to reproduce the experimentally observed pairing gaps [55]. In the RPA calculation, for the strength of the particle-hole interaction a simple mass number dependence was used, $g_{ph} = 1 + 0.002A$ [49]. For the strength of the particle-particle interaction numerical values of matrix elements are given for values of g_{pp} , which have been fitted to experimentally measured β^+/EC decay strengths [49].

As mentioned in the previous sections, in the SUSY $0\nu\beta\beta$ decay the virtually exchanged particles are assumed to be heavy. Thus, the corresponding operators will be short-ranged. For this reason the short-range part of the nuclear wave functions has to be treated carefully. In addition to the finite nucleon size effects, which are taken into account by the nucleon form factors

in momentum space (see eq. (45)), the nucleon-nucleon repulsion at short distances must be accounted for. These short-range correlations are treated by multiplying the two particle wave functions by the correlation function [56]

$$1 - f(r) = 1 - e^{-ar^2}(1 - br^2). \quad (62)$$

The two parameters a and b can be related to each other, so that effectively there is only one free parameter, the so-called correlation length defined by

$$l_c = - \int_0^\infty ds ([1 + f(r)]^2 - 1) \simeq \frac{0.748}{\sqrt{a}}, \quad (63)$$

with the standard value of $l_c = 0.7$ fm.

5.2 Numerical results and discussion

In the SUSY nuclear transition operators (46)-(47) there appear 5 basic structures (49)-(53). These, combined with the nuclear wave functions give rise to the following 5 nuclear structure matrix elements ¹

$$\mathcal{M}_{GT,N} = \langle F | \Omega_{GT,N} | I \rangle = \langle F | \sum_{i \neq j} \tau_+^{(i)} \tau_+^{(j)} \boldsymbol{\sigma}_i \cdot \boldsymbol{\sigma}_j \left(\frac{R_0}{r_{ij}} \right) F_N(x_A) | I \rangle \quad (64)$$

$$\mathcal{M}_{F,N} = \langle F | \Omega_{F,N} | I \rangle = \langle F | \sum_{i \neq j} \tau_+^{(i)} \tau_+^{(j)} \left(\frac{R_0}{r_{ij}} \right) F_N(x_A) | I \rangle \quad (65)$$

$$\mathcal{M}_{GT'} = \langle F | \Omega_{GT'} | I \rangle = \langle F | \sum_{i \neq j} \tau_+^{(i)} \tau_+^{(j)} \boldsymbol{\sigma}_i \cdot \boldsymbol{\sigma}_j \left(\frac{R_0}{r_{ij}} \right) F_4(x_A) | I \rangle \quad (66)$$

$$\mathcal{M}_{F'} = \langle F | \Omega_{F'} | I \rangle = \langle F | \sum_{i \neq j} \tau_+^{(i)} \tau_+^{(j)} \left(\frac{R_0}{r_{ij}} \right) F_4(x_A) | I \rangle \quad (67)$$

$$\mathcal{M}_{T'} = \langle F | \Omega_{T'} | I \rangle = \langle F | \sum_{i \neq j} \tau_+^{(i)} \tau_+^{(j)} \{ 3(\boldsymbol{\sigma}_i \cdot \hat{\mathbf{r}}_{ij})(\boldsymbol{\sigma}_j \cdot \hat{\mathbf{r}}_{ij}) - \boldsymbol{\sigma}_i \cdot \boldsymbol{\sigma}_j \} \left(\frac{R_0}{r_{ij}} \right) F_5(x_A) | I \rangle \quad (68)$$

¹Note, that compared to the definitions of Fermi-type matrix elements for the light neutrino case [50], [52] we took out the factor $(f_V/f_A)^2$ here. In case of the SUSY mechanism of $0\nu\beta\beta$ decay all appearing combinations of coupling constants have been absorbed into the coefficients $\alpha^{(i)}$.

We have calculated these five basic matrix elements for the experimentally most interesting isotopes. The results are given in table 2. As expected $\mathcal{M}_{GT,N}$ and $\mathcal{M}_{F,N}$ have the largest numerical values, whereas the other 3 matrix elements give only minor corrections. This can be simply understood, if one notes that matrix elements $\mathcal{M}_{GT'}, \mathcal{M}_{F'}, \mathcal{M}_{T'}$ have additional \mathbf{q}^2 factors in the integrals (59)-(60) over the momentum \mathbf{q} , transferred between two decaying neutrons. The effective nuclear cut-off for momentum transfer is $q \lesssim p_F$, where $p_F \sim 100\text{MeV}$ is the momentum of the nucleon Fermi motion inside the nucleus. This then results in the relative suppression of the nuclear matrix elements of the last three operators in eqs. (66)-(68) by factors of $(p_F/m_P)^2 \simeq$ (few) %.

The data of table 2, however, shows also another interesting fact: Corresponding matrix elements for different isotopes are relatively similar to each other, with a spread of about a factor of 2 from the mean only. As is known, much larger differences are usually found in calculations of $2\nu\beta\beta$ decay matrix elements as one goes from one isotope to another. The similarity of the SUSY $0\nu\beta\beta$ decay matrix elements is, on the other hand, not really a surprise. Recall that due to the large masses of the intermediate particles the transition operators are short-ranged. Therefore only the part of the wave functions at short distances contribute appreciably to the matrix elements and nuclear structure effects, which are so important in $2\nu\beta\beta$ decay, play a less dominant role in SUSY $0\nu\beta\beta$ decay. (See also the discussion in the next section.)

According to the eqs. (46), (47) the 5 basic matrix elements (64)-(68) can then be combined to define the following nuclear matrix elements describing contributions to $0\nu\beta\beta$ decay which correspond to *the \mathcal{R}_p SUSY mechanism*

$$\begin{aligned} \mathcal{M}_{\tilde{q}} &= \langle F | \Omega_{\tilde{q}} | I \rangle = & (69) \\ &= \frac{m_P}{m_e} \left\{ \alpha_V^{(0)} \mathcal{M}_{F,N} + \alpha_A^{(0)} \mathcal{M}_{GT,N} + \alpha_V^{(1)} \mathcal{M}_{F'} + \alpha_A^{(1)} \mathcal{M}_{GT'} + \alpha_T \mathcal{M}_{T'} \right\} \end{aligned}$$

$$\mathcal{M}_{\tilde{f}} = \langle F | \Omega_{\tilde{f}} | I \rangle = \mathcal{M}_{\tilde{q}}|_{\forall T_i=0} \quad (70)$$

and the conventional mass mechanism due to heavy Majorana neutrino exchange

$$\mathcal{M}_N = \langle F | \Omega_N | I \rangle = \frac{m_P}{m_e} \left\{ \left(\frac{f_V}{f_A} \right)^2 \mathcal{M}_{F,N} - \mathcal{M}_{GT,N} \right\}, \quad (71)$$

Table 3 shows $\mathcal{M}_{\tilde{q}}$ and $\mathcal{M}_{\tilde{f}}$ for the isotopes considered for the two sets of input parameters for the nucleon structure constants $\alpha^{(i)}$ as calculated from table 1.

Again, it is noteworthy that both sets of parameters lead to rather similar results. This is due to a partial cancellation of the differences in the input values for the $\alpha^{(i)}$, at least in the case of $\mathcal{M}_{\bar{q}}$.

Table 3 moreover shows that the $\mathcal{M}_{\bar{f}}$'s are much smaller than the $\mathcal{M}_{\bar{q}}$'s. This difference can be simply understood because only scalar and pseudoscalar currents $J_{S,P}$ contribute to $\mathcal{M}_{\bar{f}}$, but no tensor current J_T . Since in this case (see (70)) $\alpha_A^{(0)} \sim (T_1^{(3)})^2 = 0$, there is no contribution from the large $\mathcal{M}_{GT,N}$ to $\mathcal{M}_{\bar{f}}$ and consequently $\mathcal{M}_{\bar{f}} \ll \mathcal{M}_{\bar{q}}$. This result has important implications in the numerical analysis of section 6.

5.3 Uncertainties of the nuclear structure matrix elements

We have investigated the dependence of the numerical values of the matrix elements on our choice of nuclear model parameters. Besides the numerical uncertainties discussed here, there will also be deviations from the "true" matrix element due to model approximations. These, however, can not be quantified exactly. Some confidence in the model might be derived from the fact that the $2\nu\beta\beta$ decay half-life of ^{76}Ge [57] has been *predicted* correctly [49] within a factor of 2 (the $2\nu\beta\beta$ decay matrix element within $\sqrt{2}$).

In the following the three most important parameters are discussed in some detail. Other parameters, like for example g_{ph} or the use of another nucleon-nucleon potential (Reid soft-core potential [58]) instead of the Paris force have been found to have negligible effects.

In calculations of $2\nu\beta\beta$ decay [46], [47], [49] it has been shown that the $2\nu\beta\beta$ decay matrix elements calculated within pn-QRPA do strongly depend on the strength of the particle-particle interaction g_{pp} . We have therefore calculated SUSY $0\nu\beta\beta$ decay matrix elements as a function of g_{pp} for all isotopes considered in the present work. A typical example is shown in fig. 3. Compared to the results of $2\nu\beta\beta$ decay calculations only a very weak dependence of the matrix elements on g_{pp} is found. A variation of g_{pp} within ± 2 standard deviations from its fitted value [49] changes the SUSY matrix elements only by about 10 %.

²Although $\mathcal{M}_{\bar{q}}$ and $\mathcal{M}_{\bar{f}}$ are negative numerically, positive values are given in table 3. This was done to adjust the signs of matrix elements to the notation used in our previous publications on $0\nu\beta\beta$ decay in left-right-symmetric models [50], [52].

The explanation of this weak sensitivity of matrix elements on g_{pp} is similar to the one discussed in $0\nu\beta\beta$ decay calculations for light neutrino exchange [50]. Due to the selection rules for the Gamow-Teller operator, in $2\nu\beta\beta$ decay the intermediate nuclear states are 1^+ -states, exclusively. On the other hand, also higher multipoles contribute to the $0\nu\beta\beta$ matrix elements in eqs. (64)-(68) similarly to the above mentioned case of the light neutrino exchange mechanism. A typical example of a multipole decomposition for $\mathcal{M}_{GT,N}$ and $\mathcal{M}_{F,N}$ is shown in fig. 4. Quite large contributions up to high multipoles are found. Since the particle-particle force mainly affects the 1^+ -states [50], SUSY $0\nu\beta\beta$ decay matrix elements are not very sensitive to the actual choice of g_{pp} .

Figure 5 shows the nuclear matrix elements for the example of ^{130}Te as a function of the momentum cutoff factor m_A . It is seen that $\mathcal{M}_{GT,N}$, $\mathcal{M}_{F,N}$ and $\mathcal{M}_{T'}$ are rather stable against variations of m_A , while $\mathcal{M}_{GT'}$ and $\mathcal{M}_{F'}$ are more sensitive. Since $\mathcal{M}_{\bar{q}}$ is dominated by $\mathcal{M}_{GT,N}$, it will not be very sensitive to variations of m_A as well. $\mathcal{M}_{\bar{f}}$, on the other hand, has to be expected to depend more strongly on m_A .

Figure 6 then plots matrix elements as a function of the correlation length l_c for the example of ^{150}Nd . As can be read off, a 20 % change in l_c typically changes calculated $\mathcal{M}_{GT,N}$ and $\mathcal{M}_{F,N}$ by about (20 – 30) %. Similar to the case when the cutoff factor is varied, $\mathcal{M}_{GT'}$ and $\mathcal{M}_{F'}$ are found to be more sensitive to changes in l_c .

Since changes in all three parameters can lead to both larger and smaller matrix elements, the influence of a simultaneous change of these can not be estimated by simply adding up the individual errors. To estimate the total uncertainty, we have therefore calculated $\mathcal{M}_{\bar{q}}$ and $\mathcal{M}_{\bar{f}}$ at 125 grid points in this 3-dimensional parameter space. (Parameter variations within ± 20 % of their standard values for l_c and m_A and within 2 standard deviations for g_{pp} .) From this set we then calculated the "mean" matrix elements, the corresponding standard deviations and extreme values.

In case of $\mathcal{M}_{\bar{q}}$ these mean matrix elements are always very similar to those calculated for the standard values of input parameters (typical differences up to a few %). The standard deviations for $\mathcal{M}_{\bar{q}}$ and its extreme values deviate typically less than 20 % and 50 %, respectively, from the mean.

The situation is different in case of $\mathcal{M}_{\bar{f}}$. As discussed above, $\mathcal{M}_{GT'}$ shows a larger sensitivity to model parameter variations than do other matrix elements. Moreover, in case of $\mathcal{M}_{\bar{f}}$ there occurs a destructive interference between contributions from $\mathcal{M}_{F,N}$, $\mathcal{M}_{T'}$ and $\mathcal{M}_{GT'}$. In certain regions of the model parameter space $\mathcal{M}_{GT'}$ tends to cancel the contributions from the other

two matrix elements. The conclusion therefore unfortunately must be that $\mathcal{M}_{\tilde{f}}$ has to be considered to carry a large uncertainty: At extreme combinations of parameters $\mathcal{M}_{\tilde{f}}$ is smaller than (larger than) in the standard calculation by up to a factor of 5 (2).

To summarize this discussion, it can be stated that while $\mathcal{M}_{\tilde{q}}$ can be reliably calculated, the numerical value of $\mathcal{M}_{\tilde{f}}$ must be considered to be rather uncertain. Fortunately we will see in the next section that only the $\mathcal{M}_{\tilde{q}}$ matrix element is relevant for the extraction of the \mathcal{R}_p MSSM parameters from $0\nu\beta\beta$ experimental data on $0\nu\beta\beta$ decay.

6 Constraints on the \mathcal{R}_p MSSM parameter space

In the following we will analyse constraints on the \mathcal{R}_p MSSM parameter space using the experimental half-life limit of ${}^{76}\text{Ge}$, recently measured by the Heidelberg-Moscow collaboration [6] (for constraints derived from experiments on other isotopes, see below),

$$T_{1/2}^{0\nu\beta\beta}({}^{76}\text{Ge}, 0^+ \rightarrow 0^+) \gtrsim 5.6 \times 10^{24} \text{years} \quad 90\% \text{ c.l.} \quad (72)$$

The theoretical expression for the inverse $0\nu\beta\beta$ half-life (see (92)) corresponding to the reaction matrix element $\mathcal{R}_{0\nu\beta\beta}$ in eq. (39) can be written as,

$$[T_{1/2}^{0\nu\beta\beta}(0^+ \rightarrow 0^+)]^{-1} = G_{01} \left\{ (\eta_{\tilde{g}} + \eta_{\chi}) \mathcal{M}_{\tilde{q}} + (\eta_{\chi\tilde{e}} + \eta'_{\tilde{g}} - \eta_{\chi\tilde{f}}) \mathcal{M}_{\tilde{f}} + \eta_N \mathcal{M}_N \right\}^2. \quad (73)$$

In the numerical analysis we will employ for definiteness the matrix elements for Set A of the coefficients $\alpha^{(i)}$ (see table 1). Matrix elements of Set B would only yield slightly more stringent bounds, but not change any of the arguments presented below.

Neglecting for the moment the contribution from Majorana neutrino exchange (the last term in eq. (73)) we will first analyse the supersymmetric contribution alone.

Eqs. (72), (73) define an excluded area within a 5-dimensional \mathcal{R}_p MSSM parameter space

$$\{\tan \beta, \mu, m_{\tilde{g}}, m_0, \lambda'_{111}\}. \quad (74)$$

These parameters, as explained in section 2, completely define the supersymmetric particle spectrum and their interactions initiating $0\nu\beta\beta$. However, there are too many free parameters to be defined from only one constraint (eq. (72)). Fortunately, the analysis gets considerably simplified realizing that the contributions from the five different lepton number violating parameters $\eta_{\tilde{g}}, \eta_{\chi}, \eta_{\chi\tilde{e}}, \eta_{\chi\tilde{f}}, \eta'_{\tilde{g}}$ enter eq. (73) with very different magnitudes. It can be seen from eqs. (30)- (34) that

$$\eta_{\tilde{g}}, \eta'_{\tilde{g}} \gg \eta_{\chi}, \eta_{\chi\tilde{e}}, \eta_{\chi\tilde{f}} \quad \text{if} \quad m_{\tilde{q}} \sim m_{\tilde{e}}, \quad m_{\chi_i} \gtrsim 0.02m_{\tilde{g}} \quad (75)$$

with the values (28) of the gauge coupling constants α_2 and α_s and for any field composition of the neutralino states χ_i (see eq. (18)). The last mass inequality in (75) is well satisfied even for a gluino mass $m_{\tilde{g}}$ as large as 500 GeV if $m_{\chi_i} \gtrsim 20$ GeV. The latter is guaranteed by the present experimental lower bound on the lightest neutralino $\chi \equiv \chi_1$ from the LEP experiments [59] $m_{\chi} \gtrsim 20$ GeV. Later on we consider the gluino dominance more carefully and will see that it holds for $m_{\tilde{g}}$ up to 1 TeV. Another interesting fact can be derived from the nuclear matrix elements $\mathcal{M}_{\tilde{q},\tilde{f}}$ of table 3. It can be seen that the value of $\mathcal{M}_{\tilde{q}}$ is much larger than the one of $\mathcal{M}_{\tilde{f}}$. Therefore, taking into account gluino dominance eq. (75), it follows that the combination $\eta_{\tilde{g}}\mathcal{M}_{\tilde{q}}$ absolutely dominates in the half-life formula eq. (73). The advantage of this fact is twofold. First, only three \mathbb{R}_p MSSM parameters $m_{\tilde{q}}, m_{\tilde{g}}$ and λ'_{111} are involved in the numerical analysis. Second, as stated at the end of section 5, the nuclear model calculations for the matrix element $\mathcal{M}_{\tilde{q}}$ are much more reliable than those for $\mathcal{M}_{\tilde{f}}$. Thus, we are lucky to have a theoretically well controlled nuclear structure dependence in the dominant term of eq. (73). Having this in mind we proceed with the numerical analysis.

Two limiting cases are interesting to discuss: a) $m_{\tilde{d}_R} = m_{\tilde{u}_L} \equiv m_{\tilde{q}}$ and b) $m_{\tilde{u}_L} \gg m_{\tilde{d}_R} \equiv m_{\tilde{q}}$ (the case $m_{\tilde{d}_R} \gg m_{\tilde{u}_L}$ is equivalent). The following bounds are obtained

$$\text{Case a)} \quad \lambda'_{111} \leq 3.9 \times 10^{-4} \left(\frac{m_{\tilde{q}}}{100\text{GeV}} \right)^2 \left(\frac{m_{\tilde{g}}}{100\text{GeV}} \right)^{(1/2)}, \quad (76)$$

$$\text{Case b)} \quad \lambda'_{111} \leq 5.6 \times 10^{-4} \left(\frac{m_{\tilde{q}}}{100\text{GeV}} \right)^2 \left(\frac{m_{\tilde{g}}}{100\text{GeV}} \right)^{(1/2)}. \quad (77)$$

These two extreme cases differ just by a factor of $\sqrt{2}$, and for all other ratios of $(m_{\tilde{d}_R}/m_{\tilde{u}_L})$ limits between case a) and case b) are found. Motivated by the

MSSM mass formulas, eq. (19)-(24), in the following discussion we will always assume $m_{\tilde{d}_R} = m_{\tilde{u}_L}$ which corresponds to the case a).

A graphical representation of this bound (eq. (76)) is shown in fig. 7. The area on the backside of the surface is forbidden by the $0\nu\beta\beta$ decay constraint (72). Shown is the mass range between 10 GeV and 1 TeV and a coupling range between 10^{-3} and 2×10^{-1} . It is interesting to note that employing the upper bounds $m_{\tilde{q},\tilde{g}} \lesssim 1\text{TeV}$, motivated by the SUSY naturalness argument, one can obtain from (76) an upper bound for the \mathcal{R}_p Yukawa coupling constant

$$\lambda'_{111} \lesssim 0.124.$$

As mentioned before we have analysed, how the presence of a non-zero neutralino contribution to eq. (73), proportional to η_χ ,³ affects the bounds derived from eq. (76). From eq. (73), one can expect that bounds derived from $\eta_{\tilde{g}}$ would be sharpened when η_χ is switched on. The large difference in magnitude, however, leads to the result that only for very light neutralinos this effect will be of importance. This is displayed in fig. 8, where the excluded area in the $(m_{\tilde{q}}, m_{\tilde{g}}, m_\chi)$ -space is shown for the example of $\lambda'_{111} = 10^{-2}$. For a neutralino heavier than a few GeV, the squark mass and gluino mass bounds get independent of the actual value of m_χ . As can be shown, this is true for *any* neutralino composition. Since such a light neutralino mass eigenstate is already excluded by the experiments at LEP [59], which tell us that $m_\chi \geq 20$ GeV, the conclusion is that the limits of fig. 7 are practically independent of the neutralino mass.

Now another important question arises. How much will the obtained limits on superparticle masses and the \mathcal{R}_p Yukawa coupling be affected by uncertainties of the nuclear structure calculation? From the definition of the lepton number violating parameters η eqs. (30)-(34) and the $0\nu\beta\beta$ decay constraint eqs. (72)-(73) the following conclusion can be made. Any shift of the nuclear matrix element $\mathcal{M}_{\tilde{q}}$ by the value $\Delta\mathcal{M}_{\tilde{q}}$, associated with the theoretical uncertainties, would change the extracted limits on λ'_{111} , gaugino $m_{\tilde{g},\chi}$ and sfermion $m_{\tilde{q},\tilde{e}}$ masses as follows

$$\frac{\Delta m_{\tilde{g},\chi}}{m_{\tilde{g},\chi}} \sim \frac{\Delta\mathcal{M}_{\tilde{q}}}{\mathcal{M}_{\tilde{q}}}, \quad (78)$$

³Although in general all four neutralino mass eigenstates contribute to the $0\nu\beta\beta$ decay rate, it is sufficient to consider only the lightest neutralino with mass m_χ .

$$\frac{\Delta\lambda'_{111}}{\lambda'_{111}} \sim 1 - \left(1 + \frac{\Delta\mathcal{M}_{\tilde{q}}}{\mathcal{M}_{\tilde{q}}}\right)^{-\frac{1}{2}}, \quad (79)$$

$$\frac{\Delta m_{\tilde{q}}}{m_{\tilde{q}}} \sim \left(1 + \frac{\Delta\mathcal{M}_{\tilde{q}}}{\mathcal{M}_{\tilde{q}}}\right)^{\frac{1}{4}} - 1. \quad (80)$$

From these equations one can see that the limits on squark masses $m_{\tilde{q}}$ and the \mathbb{R}_p Yukawa coupling constant λ'_{111} , deduced from $0\nu\beta\beta$ decay depend only very weakly on the nuclear physics uncertainties. For instance, a change of $\mathcal{M}_{\tilde{q}}$ by even a factor of 2 changes the squark mass limit by less than 20 %.

Up to now, we have not considered the influence of a possible contribution from Majorana neutrinos to $0\nu\beta\beta$ decay. In this paper we bound ourselves to the heavy Majorana neutrino (N) contribution, as discussed at the end of sect. 2. In section 4 it was shown that contributions to $0\nu\beta\beta$ decay from the SUSY mechanism and the ordinary neutrino mass mechanism add up coherently. This is opposite to the results of [40], where a destructive interference was derived. The combined constraint in the $(m_{\tilde{q}}, m_{\tilde{g}}, \langle m_N \rangle)$ -space, where $\langle m_N \rangle$ is the *effective* heavy Majorana neutrino mass (see eq. (35)), is shown in fig. 9, for the case of $\lambda'_{111} = 10^{-2}$. It can be seen that limits on $\langle m_N \rangle$ remain valid also, if one allows contributions from supersymmetric theories to $0\nu\beta\beta$ decay (or, vice versa $0\nu\beta\beta$ decay limits on the \mathbb{R}_p MSSM are not sensitive to the actual value of the neutrino mass). This is an important result of the present work, since for a destructive interference between the neutrino mass and the SUSY mechanisms of $0\nu\beta\beta$ decay, it would always be possible to find regions in parameter space, where *no* constraints from $0\nu\beta\beta$ decay could be derived. As an interesting by-product of this analysis, we note that the current limit (72) on the $0\nu\beta\beta$ decay half-life of ^{76}Ge implies

$$\langle m_N \rangle \gtrsim 5.1 \times 10^7 \text{ GeV}. \quad (81)$$

As mentioned above, currently ^{76}Ge provides the most stringent limits on $0\nu\beta\beta$ decay. For completeness, we have calculated the limits on supersymmetric parameters in the form of eq. (76), for all isotopes considered in the present work. A summary of these limits, together with the references for the experimental half-life limits, are given in table 4.

7 Comparison of constraints from $0\nu\beta\beta$ decay with other experiments

It is interesting, to compare limits on the \mathcal{R}_p MSSM parameters from $0\nu\beta\beta$ decay, with those derived from other experiments. These constraints can be derived from low-energy processes involving virtual superparticles [15] or from direct accelerator searches. Since $0\nu\beta\beta$ decay is sensitive only to the first generation lepton number violating \mathcal{R}_p coupling, we will restrict the discussion to limits on λ'_{111} . Limits on other couplings might be found in the literature [14], [15].

In ref. [15] various low-energy processes have been analysed. It was concluded that the most restrictive limit on λ'_{111} might be derived from charged current universality. The limitation follows from the fact that the existence of \mathcal{R}_p Yukawa coupling $\lambda'_{ijk} L_i Q_j \bar{D}_k$ gives an extra contribution to quark semileptonic decays (e.g., in nuclear β decay). The effective four-fermion interaction induced by the \mathcal{R}_p MSSM contribution in fig. 10 has a $(V - A) \otimes (V - A)$ form identical to the one derived in the standard model. Therefore its contribution is equivalent to a shift in the Fermi constant G_F . If one assumes that only one \mathcal{R}_p operator has a sizable coupling constant, for instance $\lambda'_{111} L_1 Q_1 \bar{D}_1$ to a violation of charged current (CC) universality [15] because the shift of G_F is different for different generations. The experimental limits impose the following bound at the two sigma level

$$\lambda'_{111} \leq 0.03 \left(\frac{m_{\tilde{d}_R}}{100 \text{ GeV}} \right). \quad (82)$$

If one allows more than one \mathcal{R}_p operator to contribute the violation of CC universality is reduced and the above bound is weakened. Comparing (76) and (82) one can see that for masses in the range of 100 GeV, the bound (82) is less restrictive by nearly 2 orders of magnitude than the bound (76) derived from $0\nu\beta\beta$ decay.

Accelerator searches on supersymmetric particles are usually based on the assumption of R-parity conservation. In this case the LSP, which is assumed to be the neutralino χ , is stable and only weakly interacting. Therefore it escapes from the detector yielding the prominent missing transverse energy (E_T) signature of SUSY events. The CDF bounds on superparticle masses [67] rely essentially on E_T signals and are not valid in the \mathcal{R}_p case. However, in ref. [14] it has been shown that limits on superparticle masses in the \mathcal{R}_p case can be derived using the CDF dilepton search data. The corresponding mass

limit is

$$m_{\tilde{g},\tilde{q}} \geq 100\text{GeV}, \quad (83)$$

independently of λ'_{111} if $\lambda'_{111} \geq 10^{-5}$ is assumed. For smaller values of λ'_{111} , the LSP has a negligible decay probability inside the detector and the \mathcal{R}_p signal has \cancel{E}_T pattern as in the R_p conserving case. Then the limits obtained in ref. [67] can be applied for such small \mathcal{R}_p couplings. A recent calculation [26] shows that even larger masses than in eq. (83) might be probed at the TEVATRON in the near future.

There are in the literature other proposals for searching \mathcal{R}_p SUSY signals in future accelerator experiments.

The isolated like-sign dilepton signature is proposed as a characteristic feature of the \mathcal{R}_p events at the LHC

Recently searching for \mathcal{R}_p SUSY events in deep inelastic ep-scattering experiments with the ZEUS detector at HERA has been proposed [25]. Two sets of signals could be identified with these events. They are the \mathcal{R}_p resonant squark production followed by the \mathcal{R}_p cascade decay of the neutralino and the MSSM R_p conserving production of selectron and squark with their subsequent \mathcal{R}_p decay to ordinary matter. It was advocated that searching for these signals provide HERA with a promising discovery potential for \mathcal{R}_p SUSY.

A comparison of the bounds, which according to [25] might be reached with one year of HERA data, and the other limits discussed above with the limits we have obtained from the $0\nu\beta\beta$ decay constraint (72) is shown in fig. 10 in the $\lambda'_{111} - m_{\tilde{q}}$ plane. In the case of $0\nu\beta\beta$ decay, limits for 2 different values of the gluino mass are shown. It can be seen, that even for a gluino mass as large as 1 TeV which is marginal from the point of view of SUSY naturalness, the present double beta decay half-life limit yields the most restrictive bounds.⁴

To summarize this discussion, $0\nu\beta\beta$ decay allows to stringently restrict R_p violating supersymmetric theories. We have shown that these limits are more stringent than those from other low-energy processes as well as those which can be derived from the HERA experiments (see fig. 10).

8 Conclusions

We have investigated contributions to $0\nu\beta\beta$ decay from supersymmetric theories with explicit R-parity violation. The complete set of diagrams describing

⁴This result, however, does not touch upon other \mathcal{R}_p couplings than λ'_{111} which are inaccessible for $0\nu\beta\beta$, but can be probed in other processes.

quark-lepton interactions at short-distances has been considered. On this basis we have obtained the relevant low-energy effective Lagrangian in terms of nucleon and lepton currents. Then we have derived the transition operators describing $0^+ \rightarrow 0^+$ nuclear transitions induced by the \mathcal{R}_p MSSM interactions.

It has been found that contributions from the \mathcal{R}_p SUSY mechanism of $0\nu\beta\beta$ decay add coherently to the well-known neutrino mass mechanism. As a result, limits on the Majorana neutrino mass derived from $0\nu\beta\beta$ decay remain valid also if the supersymmetric contributions are taken into account.

We have calculated nuclear matrix elements of these transition operators within a realistic nuclear structure model for experimentally interesting isotopes.

Special attention has been paid to the theoretical uncertainties of the nuclear matrix elements and to the question how these uncertainties affects limits on the \mathcal{R}_p MSSM model parameters we extracted from $0\nu\beta\beta$. We were able to conclude that these limits do only very weakly depend on nuclear physics uncertainties.

Using existing experimental lower bounds on the $0\nu\beta\beta$ decay half-life $T_{1/2}$, we then analysed constraints on the \mathcal{R}_p MSSM parameters from $0\nu\beta\beta$ decay. The most restrictive limits are found from the current ^{76}Ge $0\nu\beta\beta$ decay experiment by the Heidelberg-Moscow collaboration. We conclude that $0\nu\beta\beta$ decay imposes very restrictive bounds on the lepton number violating sector of \mathcal{R}_p SUSY models. We have presented these bounds as a 3-dimensional exclusion plot in the space of the \mathcal{R}_p Yukawa coupling constant λ'_{111} , squark $m_{\tilde{q}}$ and gluino $m_{\tilde{g}}$ masses (fig.7) as well as a 2-dimensional one in the λ'_{111} - $m_{\tilde{q}}$ plane (fig.10) which also shows bounds from other low and high energy processes.

We infer that the $0\nu\beta\beta$ bounds are able to compete with or are even more stringent than those derived from current and near future accelerator experiments. Particularly, they exclude the domain which is accessible for the experiments with the ZEUS detector at HERA.

ACKNOWLEDGMENTS

We thank V.A. Bednyakov, V.B. Brudanin, M. Lindner and J.W.F. Valle for helpful discussions. The research described in this publication was made possible in part by Grant No.RFM000 from the international Science Foundation.

9 Appendix

Here we define some notations used in the main text. A complete set of the relevant formulas can be found in ref. [3].

The $0\nu\beta\beta$ reaction matrix element $\mathcal{R}_{0\nu\beta\beta}$ is defined as follows

$$\langle F|S - 1|I\rangle = 2\pi i\delta(\epsilon_1 + \epsilon_2 + E_f - E_i)\mathcal{R}_{0\nu\beta\beta} \quad (84)$$

where $E_i, E_f, \epsilon_{1,2} = \sqrt{\vec{p}_{1,2}^2 + m_e^2}$ are the energies of the initial and final nuclear states as well as the energies of two outgoing electrons with the 3-momenta \vec{p}_i .

For the Lagrangian represented in the form

$$\mathcal{L} = \frac{G_F^2}{2}m_P^{-1}\{\bar{e}(1 + \gamma_5)e^c\}\sum_i\eta_i J_i J_i, \quad (85)$$

the corresponding reaction matrix element can be written as

$$\mathcal{R}_{0\nu\beta\beta} = \frac{G_F^2}{\sqrt{2}}m_P^{-1}C_{0\nu}^{-1}\{\bar{e}(1 + \gamma_5)e^c\}\sum_i\eta_i\langle F|\Omega_i|I\rangle \quad (86)$$

The only approximation made here is that nuclear matrix elements are independent of the final-state electron energies $\epsilon_{1,2}$ and momenta $\vec{p}_{1,2}$. This approximation is well satisfied in the $0\nu\beta\beta$ decay, because $\epsilon_{1,2} \lesssim T_0 \sim (1 - 3)\text{MeV}$ (T_0 is the energy release) while the typical energy scale of the nuclear matrix elements is given by the nucleon Fermi momentum, $p_F \sim 100\text{MeV}$. Corrections to eq. (86) are smaller than 1 %.

We introduce transition operators Ω_i as

$$\langle F|\Omega_i|I\rangle = \frac{C_{0\nu}}{(2\pi)^3}\int d^3\mathbf{q}F_i^2(\mathbf{q}^2)\int d^3\mathbf{x}d^3\mathbf{y}e^{i\mathbf{q}(\mathbf{x}-\mathbf{y})}\langle F|J_i(\mathbf{x})J_i(\mathbf{y})|I\rangle. \quad (87)$$

The reaction matrix element (86) does not depend on the value of the numerical coefficient $C_{0\nu}$, which is introduced to bring the normalization of Ω in a coincidence with the literature

$$C_{0\nu} = 4\pi\frac{m_P}{m_e}\frac{R_0}{f_A^2}m_A^{-2} \quad (88)$$

The formula (87) is written for the case of heavy intermediate particles, in the closure approximation and for the outgoing electrons in S-wave states.

It is a common practice to use the non-relativistic impulse approximation (NRIA) for nuclear matrix element calculations. In this approximation the transition operator Ω_i , describing $N_a N_b \rightarrow P_a P_b$ transitions of two initial neutrons into two final protons induced by the current J_i , takes the form

$$\begin{aligned} \Omega_i = & \frac{C_{0\nu}}{(2\pi)^3} \sum_{a \neq b} \int d^3 \mathbf{q} F_i^2(\mathbf{q}^2) e^{i\mathbf{q} \cdot \mathbf{r}_{ab}} \times \\ & \times \langle P_a(\mathbf{p}_a) | J_i | N_a(\mathbf{p}'_a) \rangle_{nr} \langle N_b(\mathbf{p}_b) | J_i | N_b(\mathbf{p}'_b) \rangle_{nr} . \end{aligned} \quad (89)$$

Here $\mathbf{q} = \mathbf{p}_a - \mathbf{p}'_a = \mathbf{p}'_b - \mathbf{p}_b$ is the momentum transfer, $F_i(\mathbf{q}^2)$ are the nucleon form factors and the subscript $| \rangle_{nr}$ means non-relativistic limit for the corresponding nucleon matrix element. The summation over all pairs $N_a N_b$ of initial neutrons is implied. \mathbf{r}_{ab} is the separation between these two neutrons.

The $0\nu\beta\beta$ observables can be calculated on the basis of the reaction matrix element $\mathcal{R}_{0\nu\beta\beta}$.

The differential width of $0\nu\beta\beta$ is

$$d\Gamma = 2\pi\delta(\epsilon_1 + \epsilon_2 + E_f - E_i) \overline{|\mathcal{R}_{0\nu\beta\beta}|^2} d\Omega_1 d\Omega_2, \quad (90)$$

the phase space factors are

$$d\Omega_i = \frac{d^3 \vec{p}_i}{(2\pi)^3}. \quad (91)$$

The $0\nu\beta\beta$ half-life formula can be written as

$$[T_{1/2}^{0\nu\beta\beta}]^{-1} = \overline{|\mathcal{R}_{0\nu\beta\beta}|^2} G_{01} \quad (92)$$

where G_{01} is the leptonic phase space integral, calculated according to the prescription of [3] and has the form

$$G_{01} = \frac{a_{0\nu}}{(m_e R_0)^2 \ln(2)} \int d\Omega_1 d\Omega_2 b_{01}. \quad (93)$$

Here, $a_{0\nu} = (G_F \cos(\Theta_C) f_A / f_V)^4 m_e^9 / (64\pi^5 \hbar)$ involving only physical constants, R_0 is the nuclear radius. The kinematical factor b_{01} accounts for the Coulomb distortion of the electron waves and can be taken from ref. [3].

References

- [1] K. Grotz and H.V. Klapdor-Kleingrothaus, *The Weak Interactions in Nuclear, Particle and Astrophysics*, Adam Hilger, Bristol, New York, 1990;
- [2] W.C. Haxton and G.J. Stephenson, *Progr. Part. Nucl. Phys.* 12 (1984) 409 J. D. Vergados, *Phys. Report*, 133 (1986) 1; J.W.F. Valle, *Prog. Part. Nucl. Phys.* 26 (1991) 91. M. Moe and P. Vogel, *Annual Review of Nucl. and Part. Science* 44 (1994) 247
- [3] M. Doi, T. Kotani and E. Takasugi, *Progr. Theor. Phys. Suppl.* 83 (1985) 1;
- [4] H.V.Klapdor-Kleingrothaus in *Proc. Weak and Electromagnetic Int. in Nuclei*, Dubna, Russia 1992, World Scientific, Singapore 1993, p.201; *Nucl.Phys. (proc. Suppl.)* B31 (1993) 72; H.V.Klapdor-Kleingrothaus, *Progr.Part.Nucl.Phys.* 32 (1994) p.261.
- [5] HEIDELBERG-MOSCOW Collaboration: A. Balysh et al., *Phys. Lett. B* 283 (1992) 32 and M. Beck et al. *Phys. Rev. Lett.* 70 (1993) 2853
- [6] HEIDELBERG-MOSCOW Collaboration: A. Balysh et al., *Proceedings of the 27th Int. Conf. on High Energy Physics*, 20th-27th July 1994, Glasgow, in the press and submitted to *Phys. Lett. B*;
- [7] P. Fayet, *Nucl.Phys.* B90 (1975) 104; *Phys.Lett.* B69 (1977) 489; G.R. Farrar and P. Fayet, *Phys.Let.* B76 (1978) 575.
- [8] H.E. Haber and G.L.Kane, *Phys.Rep.* 117 (1985) 75; H.P. Nilles, *Phys.Report.* 110 (1984) 1.
- [9] S. Dimopoulos and L.J. Hall, *Phys.Lett.* B207 (1987) 210.
- [10] L. Hall and M. Suzuki, *Nucl.Phys.* B 231 (1984) 419.
- [11] E. Ma and D. Ng, *Phys. Rew.* D41 (1990) 1005,
- [12] C. Aulakh and R. Mohapatra, *Phys.Lett.* B119 (1983) 136; G.G. Ross and J.W.F. Valle, *Phys.Lett.* B151 (1985) 375; J. Ellis et al., *Phys.Lett.* B150 (1985) 142; A. Santamaria and J.W.F. Valle, *Phys.Lett.* B195 (1987) 423; *Phys.Rev.Lett.* 60 (1988) 397; *Phys.Rev.* D 39 (1987) 1780; M.C. Gonzalez-Garsia and J.W.F. Valle, *Nucl.Phys.* B355 (1991) 330; J.W.F. Valle, *Phys.Lett.* B196 (1987) 157;

- [13] A. Masiero and J.W.F. Valle Phys.Lett. B251 (1990) 273.
- [14] D.P. Roy, Phys. Lett. B 283 (1992) 270.
- [15] V. Barger, G.F. Giudice and T. Han, Phys. Rev. D 40 (1989) 2987
- [16] F. Zwirner, Phys. Lett. B132 (1983) 103.
- [17] S. Weinberg, Phys.Rev. D26 (1982) 287;
- [18] R. Barbieri and A. Masiero, Nucl.Phys. B267 (1986) 679;
- [19] A. Bouquet and P. Salati, Nucl.Phys. B284 (1987); A. Nelson and S.M. Barr, Phys.Lett. B258 (1991) 45;
- [20] B.A. Campbell, S. Davidson, J. Ellis and K. Olive, Phys.Lett. B256 (1991) 457; CERN-preprint, CERN-TH-6208-91; W. Fieschler, G. Giudice, R.G. Leigh and S. Paban, Phys.Lett. B258 (1991) 45.
- [21] S. Dimopoulos and L.J. Hall, Phys.Lett. B196 (1987) 135; R. Mohapatra and J.W.F. Valle, Phys.Lett. B186 (1987) 303; J. Cline S. Rabby Ohio State preprint,1990.
- [22] H. Dreiner and G. Ross, Nucl. Phys. B 410 (1994) 188.
- [23] J.L. Hewett, Contrib. to Proc. of 1990 Summer Study on High Energy Physics (Snowmass, Colorado).
- [24] H. Dreiner and G. Ross, Nucl. Phys. B 365 (1991) 597.
- [25] J. Butterworth and H. Dreiner, Nucl. Phys. B 397 (1993) 3;
- [26] H. Baer, C. Kao and X. Tata, hep-ph/9410283; and FSU-HEP-941001
- [27] R.M. Godbole, P. Roy and X. Tata, Nucl.Phys. B401 (1993) 67;
- [28] H. Dreiner, M. Gauchait and D.P.Roy, Phys.Rev. D 49 (1994) 3270;
- [29] S. Dimopoulos, S. Raby and F. Wilczek, Phys.Lett. B112 (1982) 133.
- [30] N. Sakai and T. Yanagida, Nucl.Phys. B197 (1982) 83;
- [31] D. Braham and L. Hall, Phys.Rev. D40 (1989) 2449;

- [32] M. Bento, L.J. Hall and G.G. Ross, Nucl.Phys. B292 (1987) 400; G. Lazarides, P.K. Mohapatra, C. Panagiotakopoulos and Q. Shafi, Nucl.Phys. B323 (1989) 614;
- [33] L.E.Ibañez and C.Lopez, Phys.Lett. B126 (1983) 54; Nucl.Phys. B233 (1984) 511; L.E.Ibañez, C. Lopez and C.Muñoz, Nucl.Phys. B256 (1985) 218; K.Inoue, A.Kakuto, H.Komatsu and S. Takeshita, Progr.Theor.Phys. 68 (1982) 927; 71 (1984) 348.
- [34] L.E.Ibañez and G.G.Ross, CERNTH-6412-92, to appear in *Perspectives on Higgs Physics*, ed. by G.Kane, p.229 and references therein; J.Ellis, G.L. Fogli and E. Lisi, Nucl.Phys. B393 (1993) 3; M.Drees and M.M.Nojiri, Nucl.Phys. B369 (1992) 54.
- [35] J.F. Gunion, H.E. Haber, G.L. Kane, Nucl.Phys. B 272 (1986) 1.
- [36] J. Ellis, J. Hagelin, D.V. Nanopoulos, K. Olive and M. Sredniki, Nucl.Phys. B238 (1984) 453.
- [37] I. H. Lee, Nucl. Phys. B 246 (1984) 120. R. Mohapatra, S. Nussinov and J.W.F. Valle, Phys.Lett. B165 (1985) 417. R. Barbieri et al. Phys. Lett. B 238 (1990) 86.
- [38] M. Hirsch, H.V. Klapdor-Kleingrothaus and S.G. Kovalenko submitted to Phys.Lett. B.
- [39] R. Mohapatra, Phys.Rev. D34 (1986) 3457.
- [40] J.D Vergados, Phys.Lett. B184 (1987) 55;
- [41] J.L. Lopez, D.V. Nanopoulos and K. Yuan, Nucl. Phys. B370 (1992) 445; J. Ellis and L. Roszkowski, Phys. Lett. B283 (1992) 252; L.Roszkowski, Phys.Lett. B262 (1991) 59; *ibid* B278 (1992) 147; K.Griest and L.Roszkowski, Phys.Rev. D46 (1992) 3309. R.G.Roberts, L.Roszkowski, Phys.Lett. B309 (1993) 329; M.Drees and M.M.Nojiri, Phys.Rev. D47 (1993) 376.
- [42] J. Erler and P. Langacker, UPR-0632T.
- [43] S.L. Adler et al., Phys.Rev. D11 (1975) 3309;

- [44] J.D. Vergados, Phys.Rev. C24 (1981) 640; J.D. Vergados, Nucl.Phys. B218 (1983) 109.
- [45] J.A. Halbleib and R.A. Sorenson, Nucl. Phys. A 98 (1967) 542
- [46] P. Vogel and M.R. Zirnbauer, Phys. Rev. Lett. 57 (1986) 3148 and J. Engel, P. Vogel, M.R. Zirnbauer, Phys. Rev. C 37 (1988) 731
- [47] O. Civitarese, A. Faessler and T. Tomoda, Phys. Lett. B 194 (1987) 11, T. Tomoda, A. Faessler, Phys. Lett. B 199 (1987) 475, J. Suhonen, T. Taigel and A. Faessler, Nucl Phys. A 486 (1988) 91
- [48] K. Muto and H.V. Klapdor, in: *Neutrinos*, ed. H.V. Klapdor, Springer, Heidelberg, New York, 1988, p. 183
- [49] K. Muto, E. Bender and H.V. Klapdor, Z. Phys. A 334 (1989) 177
- [50] K. Muto, E. Bender and H.V. Klapdor, Z. Phys. A 334 (1989) 187
- [51] M. Hirsch, X.R. Wu, H.V. Klapdor-Kleingrothaus, C.R. Ching and T.H. Ho, Z. Phys. A 345 (1993) 163
- [52] M. Hirsch, K. Muto, T. Oda and H.V. Klapdor-Kleingrothaus, Z. Phys. A 347 (1994) 151
- [53] A. Bohr and B.R. Mottelson, Nuclear Structure, Vol. 1, Benjamin, New York, 1969
- [54] M. Lacombe, B. Loiseau, J.M. Richard, R. Vinh Mau, J. Côté, P. Pires and R. de Tournel, Phys. Rev. C21 (1980) 861 and N. Anantaraman, H. Toki and G.F. Bertsch, Nucl. Phys. A 398 (1983) 269
- [55] A.H. Wapstra, G. Audi and R. Hoekstra, At. Data Nucl. Data Tables 39 (1988) 281
- [56] G.A. Miller and J.E. Spencer, Ann. Phys. 100 (1976) 562
- [57] A. Balysh et al., Phys. Lett. B 322 (1994) 176
- [58] R.V. Reid, Ann. Phys. (N.Y.) 50 (1968) 411
- [59] L. Roszkowski, Phys.Lett. B252 (1990) 471; K. Hidaka, Phys.Rev. D44 (1991) 927; Review of Particle Properties, Phys.Rev. D45, No.11 (1992) S1.

- [60] T. Bernatowicz et al., Phys. Rev. Lett. 69 (1992) 2341
- [61] S.R. Elliott et al., Phys. Rev. C 46 (1992) 1535
- [62] A. Alessandrello et al., Phys. Lett. B 335 (1994) 519
- [63] M. Alston-Garnjost et al., Phys. Rev. Lett. 71 (1993) 831
- [64] J.-L. Vuilleumier et al., Phys. Rev. D 48 (1993) 1009
- [65] H.Ejiri et al., Progr. Part. Nucl. Phys. 32 (1994) 119
- [66] M.K. Moe et al., Progr. Part. Nucl. Phys 32 (1994) 247
- [67] Talks given by J.T.White (D0 collaboration) and by Y.Kato (CDF collaboration) at 9th Topical Workshop on Proton-Antiproton Collider Physics, Tsukuba, Japan, October, 1993.

Figure Captions

- Fig.1a Basic diagram for neutrinoless double beta decay.
- Fig.1b Basic diagram for neutrinoless double beta decay at the quark level.
- Fig.2a Feynman graphs for the conventional mechanism of $0\nu\beta\beta$ decay by massive Majorana neutrino exchange.
- Fig.2b Feynman graphs for the supersymmetric contributions to $0\nu\beta\beta$ decay.
- Fig.2c New "non-diagonal" Feynman graphs for supersymmetric contributions to $0\nu\beta\beta$ decay [38].
- Fig.3a SUSY $0\nu\beta\beta$ decay matrix elements as a function of the particle-particle strength g_{pp} , for the example of ^{76}Ge . Shown are $M_{GT,N}$ (full line) and $M_{F,N}$ (dashed line).
- Fig.3b As fig. 3.a, but for $\mathcal{M}_{GT'}$ (full line) and $\mathcal{M}_{F'}$ (dashed line) and $\mathcal{M}_{T'}$ (dash-dotted line).
- Fig.4 Multipole decomposition of the matrix elements $\mathcal{M}_{GT,N}$ and $\mathcal{M}_{F,N}$ for the example of ^{76}Ge .

- Fig.5a Matrix elements $\mathcal{M}_{GT,N}$ (full line) and $\mathcal{M}_{F,N}$ (dashed line) for ^{130}Te as a function of the momentum cutoff factor m_A [MeV].
- Fig.5b As fig. 5.a, but for $\mathcal{M}_{GT'}$ (full line) and $\mathcal{M}_{F'}$ (dashed line) and $\mathcal{M}_{T'}$ (dash-dotted line).
- Fig.6a Matrix elements $\mathcal{M}_{GT,N}$ (full line) and $\mathcal{M}_{F,N}$ (dashed line) for ^{150}Nd as a function of the correlation length l_C [fm].
- Fig.6b As fig. 6.a, but for $\mathcal{M}_{GT'}$ (full line) and $\mathcal{M}_{F'}$ (dashed line) and $\mathcal{M}_{T'}$ (dash-dotted line).
- Fig.7 Constraints from $0\nu\beta\beta$ decay on the squark $m_{\tilde{q}}$ and gluino $m_{\tilde{g}}$ masses and the R-parity violating Yukawa coupling constant λ'_{111} . Values on the backside of the surface are forbidden by non-observation of $0\nu\beta\beta$ decay. $m_{\tilde{d}_R} = m_{\tilde{u}_L} = m_{\tilde{q}}$ is assumed and the matrix element $\mathcal{M}_{\tilde{q}}$ for Set A of the coefficients $\alpha^{(i)}$ has been used.
- Fig.8 Dependence of the squark and gluino mass limits derived from $0\nu\beta\beta$ decay on the actual value of the neutralino mass m_χ for $\lambda'_{111} = 10^{-2}$.
- Fig.9 Combined limits on supersymmetric particle masses $m_{\tilde{q},\tilde{g}}$ and the effective heavy Majorana neutrino mass $\langle m_N \rangle$ for $\lambda'_{111} = 10^{-2}$.
- Fig.10 Feynman graph for neutron decay in R_p -violating supersymmetric theories, see text.
- Fig.11 Comparison of limits on R-parity violating supersymmetric theories from different experiments in the $(m_{\tilde{q}}-\lambda'_{111})$ plane. The dashed line is the limit from charged-current universality according to [15]. The vertical line is the lower limit on squark masses in R_p -violating supersymmetric theories from the TEVATRON, according to [14]. The thick full line is the region which might be explored by HERA with about one year of data [25]. The 2 full lines to the right are the limits obtained from non-observation of the $0\nu\beta\beta$ decay of ^{76}Ge for gluino masses of (from left to right) $m_{\tilde{g}} = 1$ TeV, 100 GeV, respectively. The parameter regions to the upper left of the lines are forbidden by the different experiments. It is seen that even for a gluino mass as large as 1 TeV, $0\nu\beta\beta$ decay gives the most stringent limits.

Table 2: Nuclear matrix elements for SUSY $0\nu\beta\beta$ decay for the experimentally most interesting isotopes calculated within pn-QRPA. $\mathcal{M}_\alpha \times 10^x$ implies that the matrix element should be divided by 10^x to get the correct numerical value. These factors are introduced here, just to show the differences in magnitude of the different matrix elements.

^AY	$\mathcal{M}_{GT,N} \times 10^1$	$\mathcal{M}_{F,N} \times 10^2$	$\mathcal{M}_{GT'} \times 10^3$	$\mathcal{M}_{F'} \times 10^3$	$\mathcal{M}_{T'} \times 10^3$
^{76}Ge	1.13	-4.07	-7.70	3.06	-3.09
^{82}Se	1.02	-3.60	-7.13	2.76	-2.76
^{100}Mo	1.29	-4.89	-7.88	3.52	-4.93
^{116}Cd	0.75	-2.71	-5.49	2.19	-2.65
^{128}Te	1.19	-4.19	-7.95	3.11	-3.85
^{130}Te	1.05	-3.69	-6.97	2.73	-3.53
^{136}Xe	0.58	-2.03	-3.81	1.49	-1.81
^{150}Nd	1.65	-5.91	-10.4	4.32	-7.51

Table 3: Nuclear matrix elements for SUSY $0\nu\beta\beta$ decay. Shown are $\mathcal{M}_{\tilde{q}}$ and $\mathcal{M}_{\tilde{f}}$ for the two sets of input values of coefficients for the $\alpha^{(i)}$ of table 1.

${}^A\text{Y}$	A) $\mathcal{M}_{\tilde{q}}$	B) $\mathcal{M}_{\tilde{q}}$	A) $\mathcal{M}_{\tilde{f}}$	B) $\mathcal{M}_{\tilde{f}}$
${}^{76}\text{Ge}$	283	304	13.2	20.7
${}^{82}\text{Se}$	253	272	11.3	17.9
${}^{100}\text{Mo}$	328	356	23.6	33.5
${}^{116}\text{Cd}$	190	205	11.0	16.2
${}^{128}\text{Te}$	298	323	16.7	24.8
${}^{130}\text{Te}$	262	284	15.4	22.5
${}^{136}\text{Xe}$	143	155	7.91	11.8
${}^{150}\text{Nd}$	416	456	34.4	47.0

Table 4: Comparison of limits on supersymmetric parameters derived from different $\beta\beta$ decay experiments (see quoted references for half-life limits), written in the form of eq. (76):

$$\lambda'_{111} \leq \epsilon \left(\frac{m_{\tilde{g}}}{100\text{GeV}} \right)^2 \left(\frac{m_{\tilde{g}}}{100\text{GeV}} \right)^{(1/2)}.$$

Currently ^{76}Ge provides the most stringent limits. ([Ref.] ^a 90 % c.l., whereas [Ref.] ^b 68 % c.l. only.)

^AY	ϵ	Ref.	^AY	ϵ	Ref.
^{76}Ge	3.9×10^{-4}	[6] ^a	^{128}Te	4.9×10^{-4}	[60] ^b
^{82}Se	1.1×10^{-3}	[61] ^b	^{130}Te	1.1×10^{-3}	[62] ^a
^{100}Mo	7.5×10^{-4}	[63] ^b	^{136}Xe	6.8×10^{-4}	[64] ^a
^{116}Cd	2.5×10^{-3}	[65] ^a	^{150}Nd	9.7×10^{-4}	[66] ^a

Figure 1.a

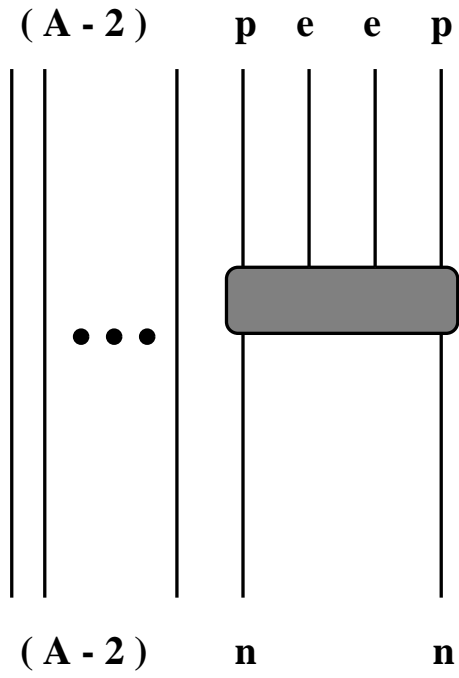


Figure 1.b

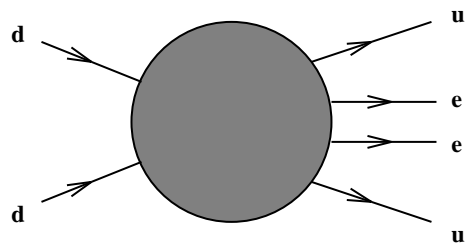


Figure 2.a

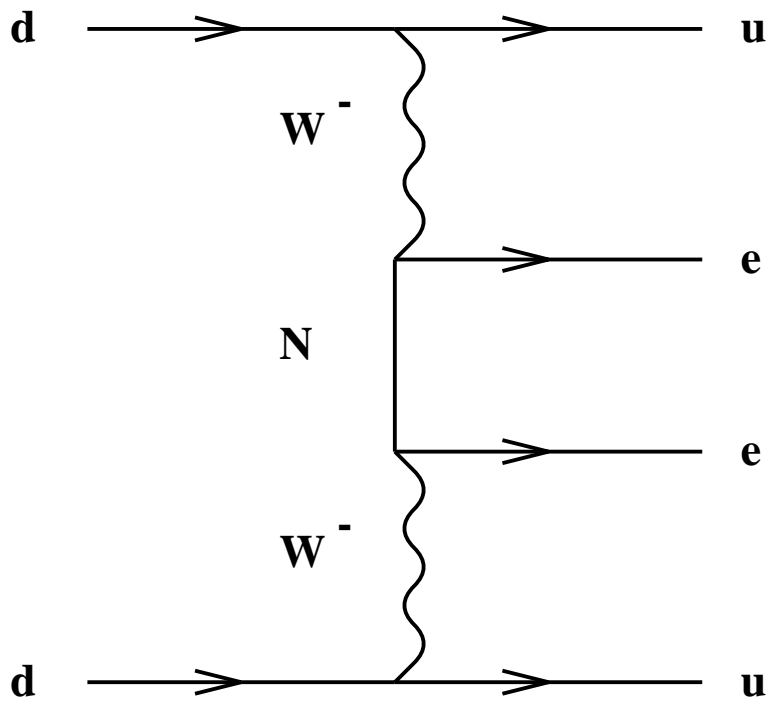


Figure 2.b

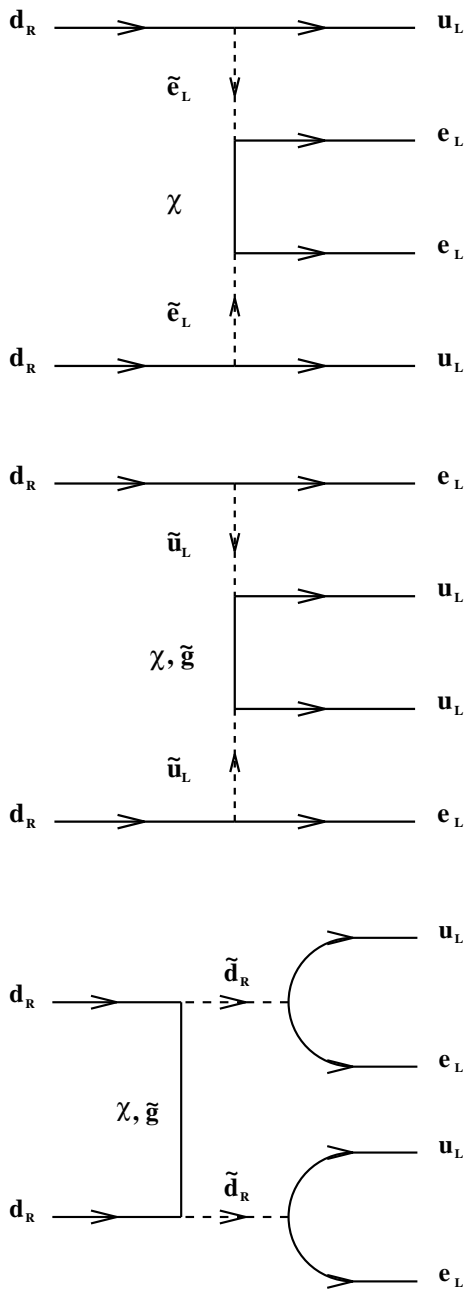


Figure 2.c

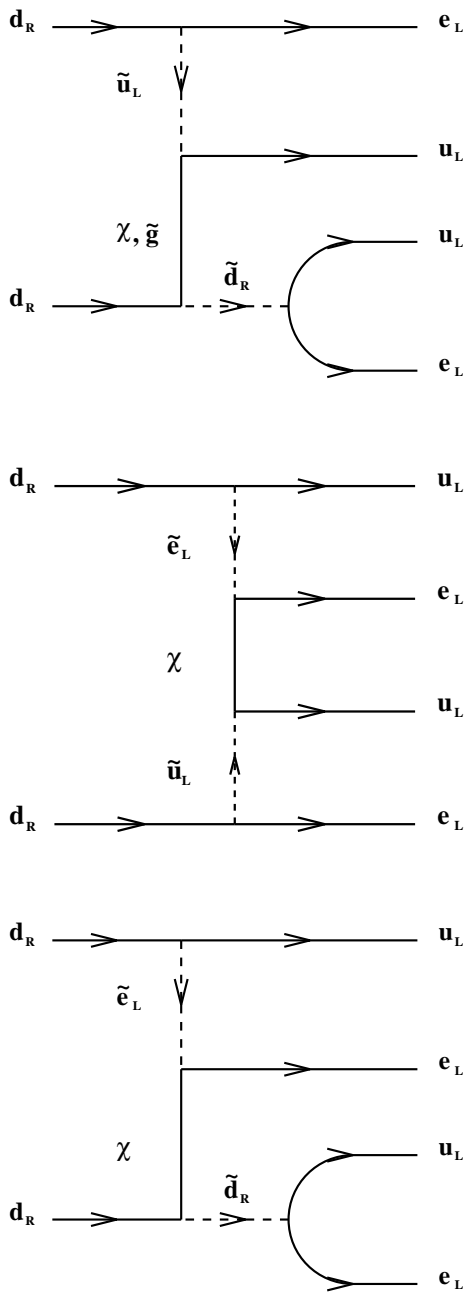


Figure 3.a

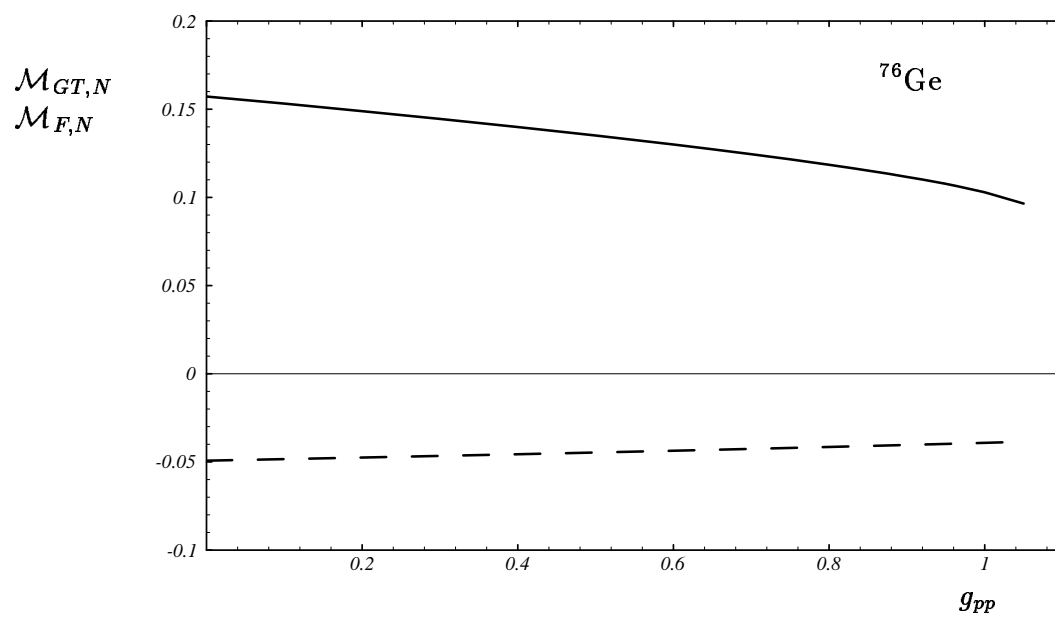


Figure 3.b

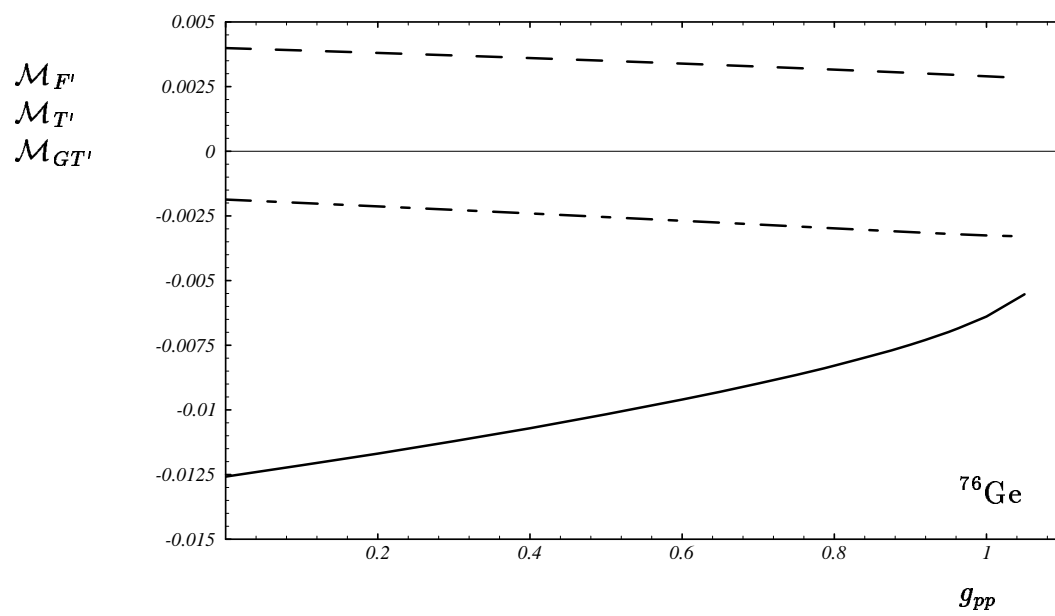


Figure 4

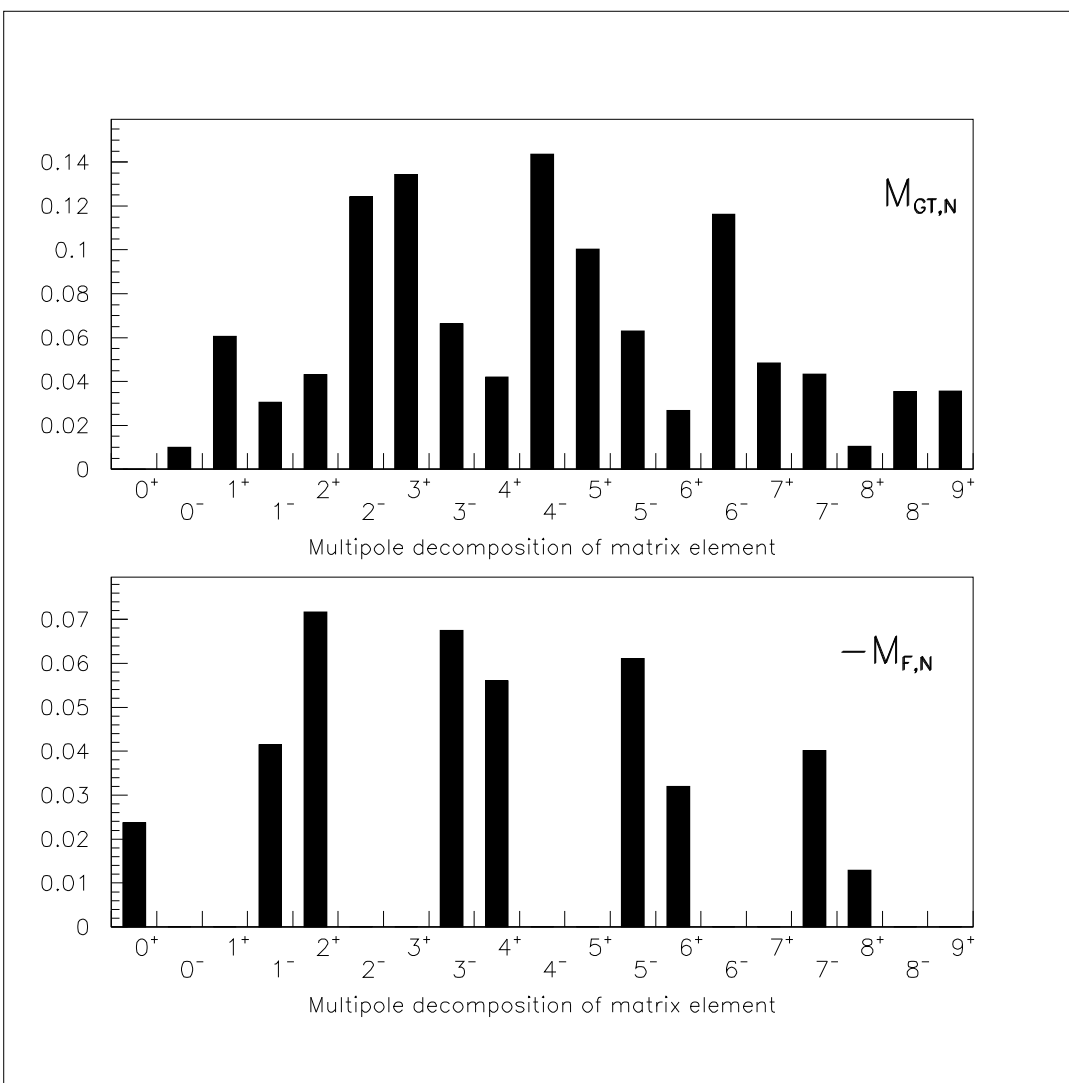


Figure 5.a

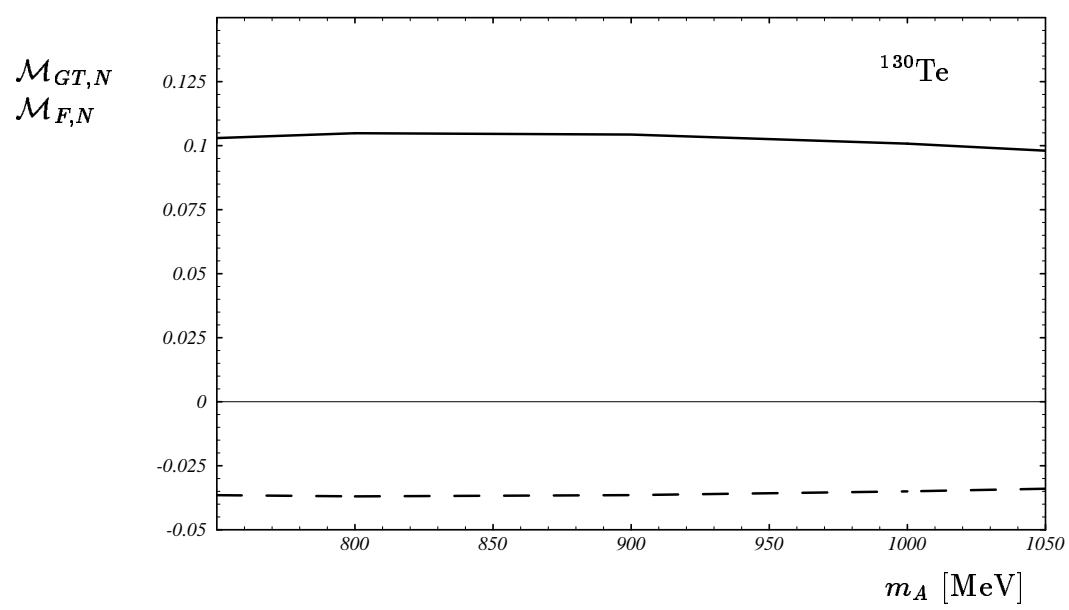


Figure 5.b

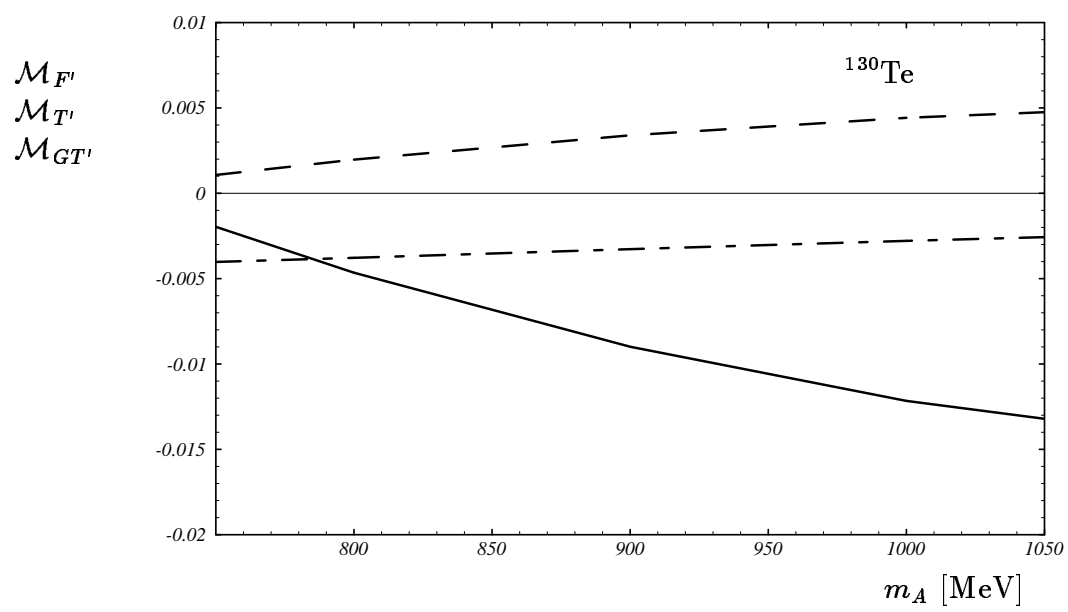


Figure 6.a

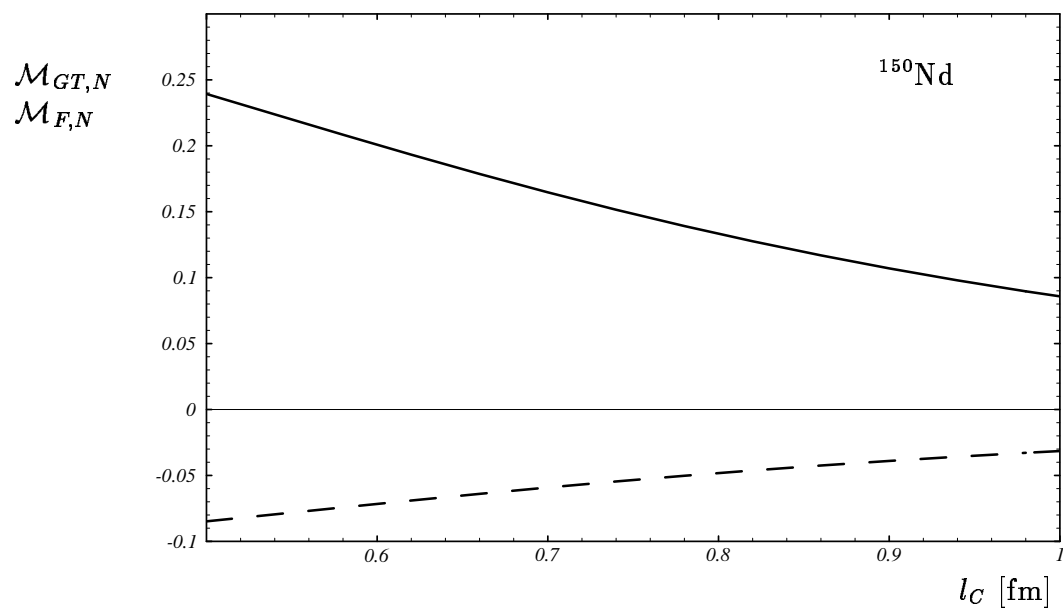


Figure 6.b

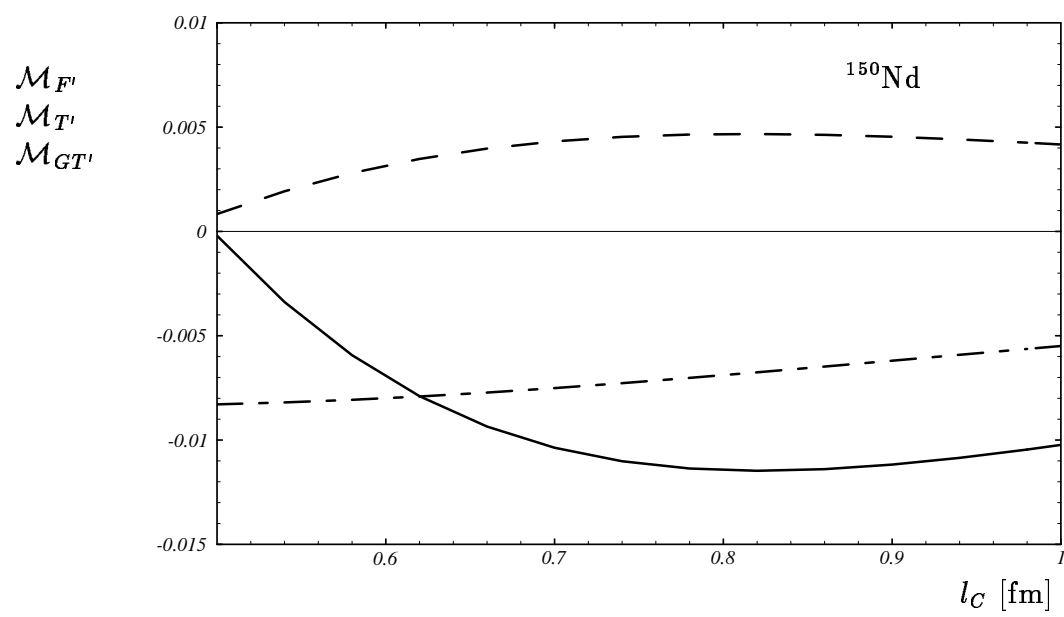


Figure 7

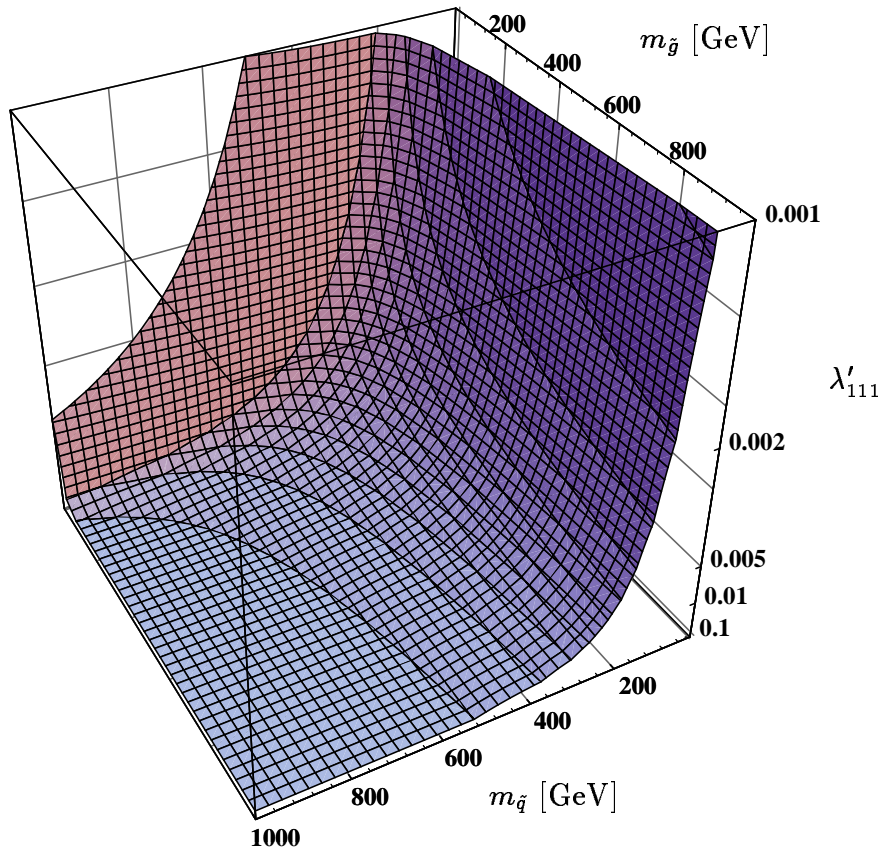


Figure 8

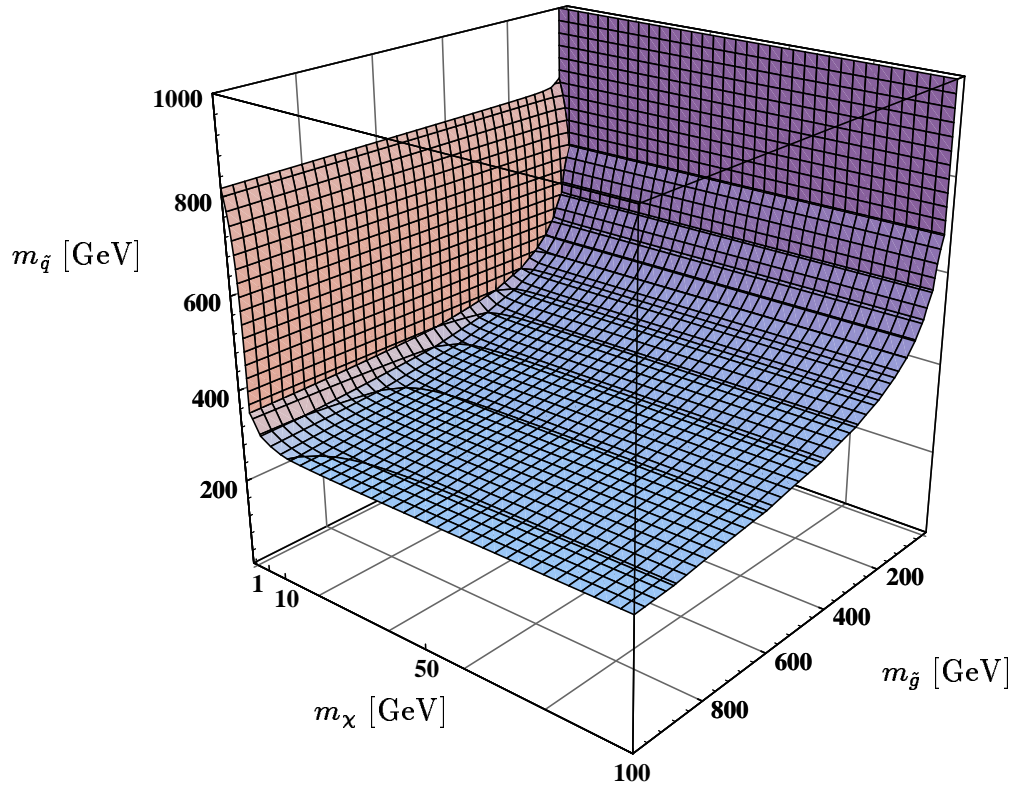


Figure 9

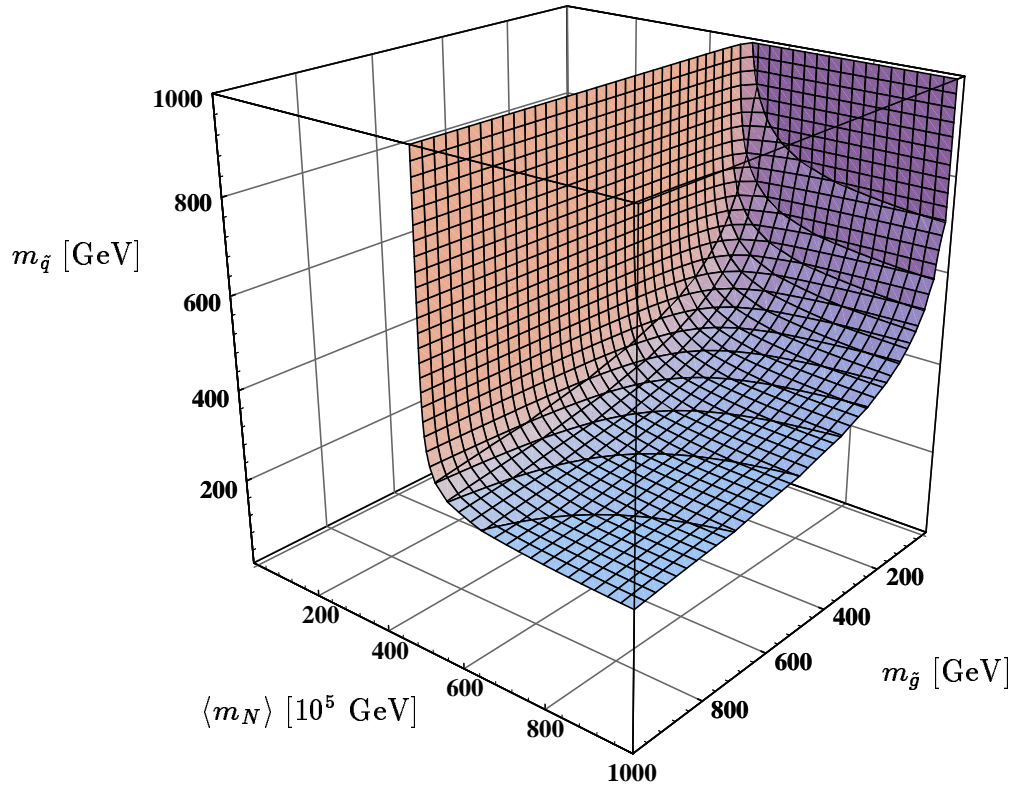


Figure 10

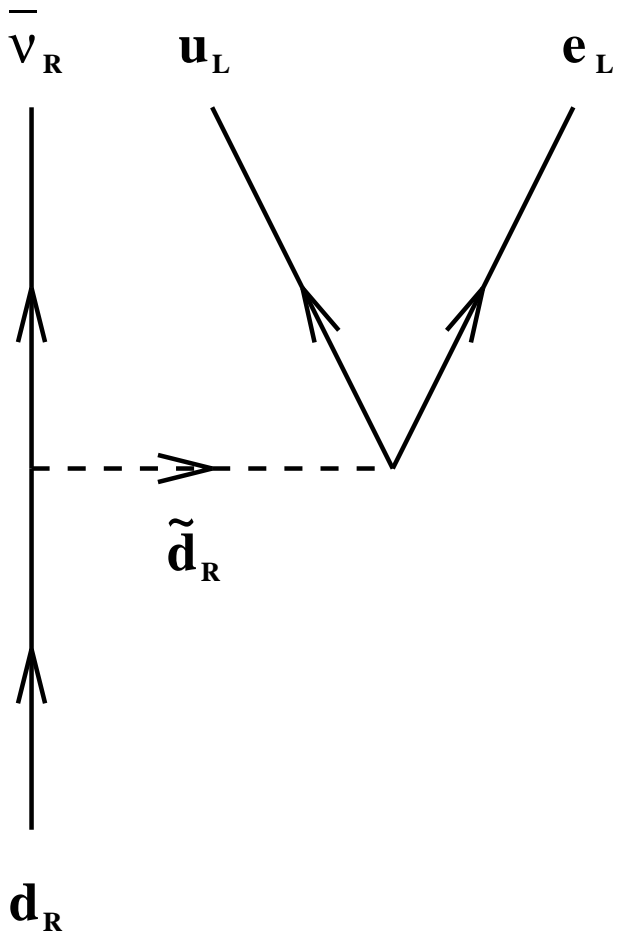


Figure 11

